Remote Sensing Based Assessment of Biophysical Indicators for Land Degradation and Desertification

S.L. Ustin[1,2], S. Jacquemoud[3], A. Palacios-Orueta[1,4], L. Li[5], and M.L. Whiting[1]
[1]California Space Institute Center of Excellence, University of California
Davis, CA 95616, USA, email slustin@ucdavis.edu
[2]Department of Geography and Environmental Science, University of Auckland, New Zealand
[3]Institut de Physique du Globe de Paris, Géodésie & Gravimétrie, 4 Place Jussieu,
75252 Paris Cedex 5, France
[4] Departamento de Silvopascicultura, Universidad Politécnica de Madrid, Spain
[5]Department of Geology, Indiana University-Purdue University, Indianapolis, IN USA

ABSTRACT

Desert ecosystems spanning moisture conditions from dry grasslands to barren hyper-arid landscapes are the largest terrestrial biome with more than 40% of the terrestrial landmass. Remote sensing data provide an efficient cost-effective means to assess biophysical indicators of land degradation and desertification, providing that essential ecosystem properties can be monitored. We review the spectral characteristics of plants and soils that are detectable using optical sensors and methods to identify and quantify properties that have potential for monitoring arid ecosystem processes. Vegetation indexes have little sensitivity at low leaf area, particularly when the soil background is highly variable, as is characteristic of many arid systems. Additionally, accumulated dry plant material on the soil surface challenges measurement. Although the absorption characteristics of the major biochemical constituents of plants and soils are generally understood, the methods to retrieve this information from reflectance data and to understand the significance of how the structural organization alters the absorption features remains an area of active research. The overlapping absorption features of plants and soils preclude direct assessment of many biogeochemicals of interest. New biophysical methods that take the full spectral shape into account, including the effect of one compound on the spectral absorption of another, are needed to reduce uncertainty in their estimates. As a result, despite significant progress in developing fundamental understanding of ecosystem processes and optical properties, more research is needed before fully predictable quantitative methods are available.

Keywords: spectral indexes, biophysical indicators, radiative transfer, reflectance models

1 INTRODUCTION: DESERTS AND DESERTIFICATION

Desert and dryland ecosystems, including hyperarid, arid, semiarid, and dry subhumid areas are the largest terrestrial biome, about 41% of the terrestrial landmass [1]. Deserts are categorized by precipitation with extremely arid lands having at least 12 consecutive months without precipitation, arid lands having less than 250 mm annual rainfall, and semiarid lands having mean annual precipitation between 250 and 500 millimeters [2]. Arid and extremely arid lands are deserts, and semiarid and dryland ecosystems are generally grassland or savanna. Deserts have evolved into their modern distributions (Figure 1) largely in response to Quaternary climate conditions, superimposed on local environmental factors. Present desert expansion is attributed to land degradation from land use, land use change, and climate change [1]. There is growing evidence that human activities are creating unprecedented rates of ecosystem change such that novel combinations of climate and disturbance factors may perhaps exceed the capacity of current ecosystems to adapt. Desert ecosystems are typically fragile and even small perturbations can have long-lasting impacts on the distribution of vegetation and on functionality of the landscape [3-4]. Vegetation change may have positive feedbacks to climate that accelerate change [5]. Conversely, within the historic range of climate, vegetation distributions tend to be stable, despite large inter-annual variability [6].

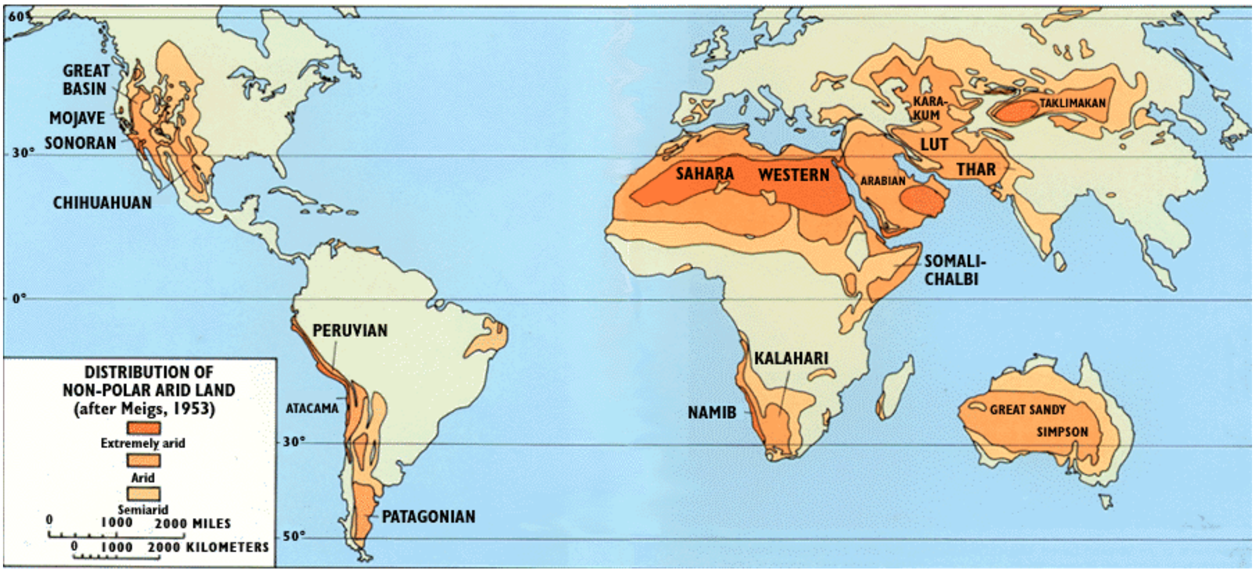

Figure 1. Global distribution of arid ecosystems [1].

Desertification is defined as "land degradation in arid, semiarid, and dry subhumid areas resulting from various factors, including climatic variations and human activities" [1], where *land degradation* is defined as reduction or loss of biological or economic productivity. [7] identified three processes that promote desertification: 1) deterioration of vegetation cover from overgrazing, wood cutting and burning; 2) wind and water erosion from improper land management; and 3) salinization from improper irrigation management. Desertification affects all continents (except Antarctica), and 10-20% of global arid systems are believed to be degraded. Because nearly one-third of the human population lives in arid regions, the threat of desertification ranks among the most important environmental problems and has significant impacts on meeting human well-being.

Many interacting factors affect the ecosystem sustainability and resistance to degradation (Figure 2). Maintenance of the biotic composition, diversity, and cover is essential to sustainable productivity. In addition to plant factors, maintenance of soil quality processes, including soil texture, nutrient, and biogeochemical cycles, soil microorganisms and biological crust, and resistance to wind and water borne erosion is also essential to sustaining the health of the ecosystem. Changes in vegetation characteristics and shifts in phonological cycles may accelerate impacts from climate variability and land use. To protect arid lands from accelerated desertification and reduce the potential for feedbacks that may accelerate global climate changes, it is important to understand these integrated ecosystem responses.

Deserts and semi-arid ecosystems are by definition limited by water. Low but highly variable precipitation, often with unpredictable periodicity, dominates the responses of desert ecosystems [8-10]. Fractional cover, biomass and leaf area are generally proportional to precipitation and available soil moisture [11]. Life forms shift depending on the predictability of precipitation, with grasses more abundant under predictable precipitation regimes and shrublands dominating when rainfall becomes more irregular in timing and amount [3],[10],[12]. A primary driver of desertification is loss of vegetative cover which creates a positive feedback to lower precipitation [13]. Desert ecosystems are often secondarily limited by nutrients, particularly nitrogen [14]. In contrast, nitrogen deposition along with CO_2 enrichment is likely to enhance growth and affect other ecosystem attributes like species composition, growth form, and phonological patterns [14]. Enhanced growth may also alter delicately balanced desert ecosystem functions—changing nutrient, fire and water cycles. Conditions that favor succession may promote invasion by exotic species. A landmark study by Schlesinger et al. [3] showed a progressive pattern of desertification occurred as soil nutrients became less uniformly distributed as an ecosystem transformed from grassland to desert shrubland, that lead to unproductive barren soil between islands of higher fertility. How deserts will respond to multiple simultaneous environmental changes becomes highly uncertain. An increase in inter-annual climate variability (e.g., El Niño precipitation) could under multiple stressor conditions, exceed a threshold and produce a step change in ecosystem structure and function [5].

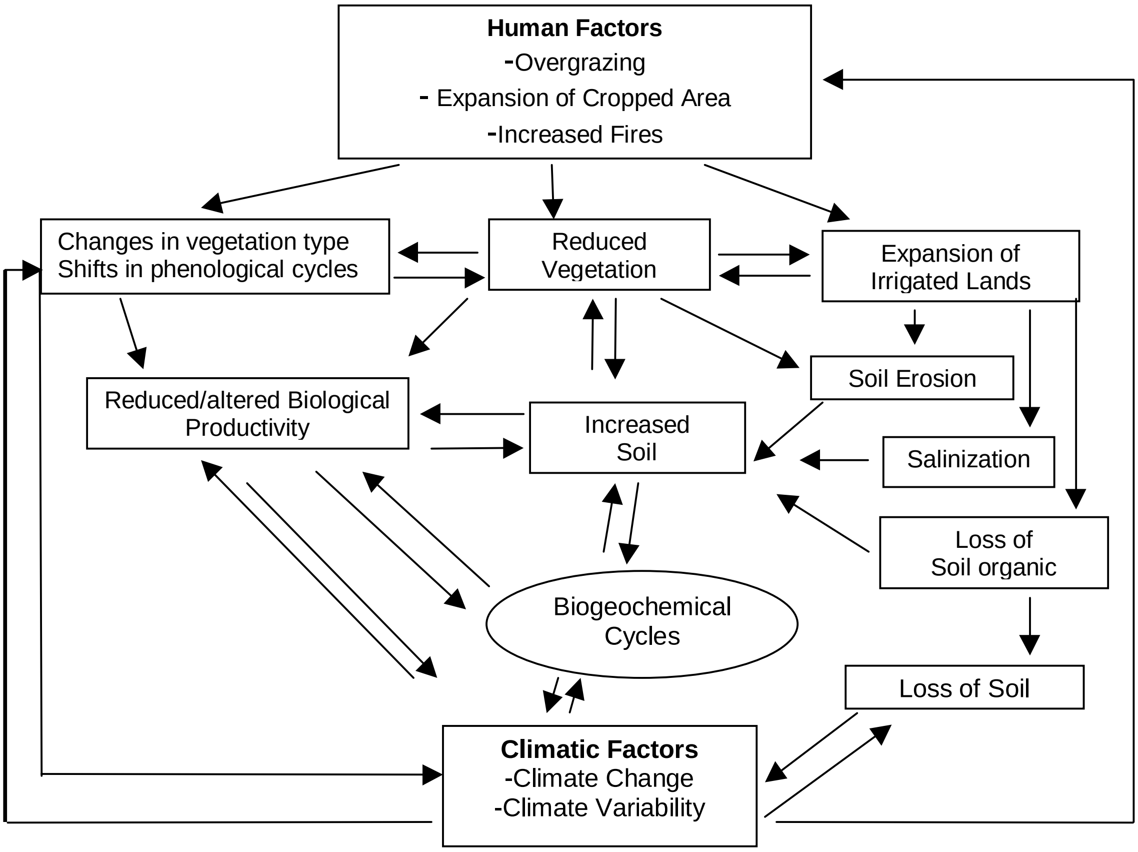

Figure 2. Interactions among climate and human activities that affect functioning of arid ecosystems.

The first few centimeters of soil are the most fertile and most susceptible to rain and wind erosion. Improved ability to quantify and monitor soil properties, especially soil surface chemistry, can provide key indicators of desertification. Knowledge of the distribution of secondary clay and organic matter will contribute to understanding plant and soil responses in arid regions and also contribute to monitoring desertification. Mapping of clay and organic matter will improve estimates of soil carbon, a key parameter for developing an understanding of the impacts of altered rainfall distributions, deposition of pollutants, and increases in greenhouse gas concentrations. Of particular concern for desertification from climate change is the formation and dissolution of pedogenic inorganic carbon. Despite the fact that the global inorganic carbon pool is comparable in size to the pool of atmospheric CO_2 and to soil organic carbon, there has been little research on the impact of changing hydrologic processes on this pool of inorganic carbon.

2 RETRIEVING BIOPHYSICAL SPECTRAL INFORMATION

2.1 Biophysical Information from Living Plants

Desert species have developed convergences in the types of leaf structures they have evolved. Similarly, growth forms converge, typically limited to grasses and drought-tolerant shrubs. Plant cover is the most obvious indicator of precipitation and soil moisture status. Numerous studies have shown a strong linear relationship between plant cover, biomass, and leaf area in response to water availability [6]. Typically, leaf traits include small thick leaves, with thick cuticles and pubescence, sunken stomates, and small mesophyll cells with thick cell walls and small air spaces. The reflectance and transmittance of leaves is a function of both the concentration of light absorbing compounds (chlorophyll, water, dry plant matter, etc.) and the surface/internal scattering of light that is not efficiently absorbed (Figure 3). Leaf absorbance is reduced by pubescence, and leaves appear more reflective after the hairs have dried out [15],[16]. As the properties of xeromorphic plant leaves change, e.g., they become more schlerophyllous (drought hardened) or desiccated, and reflectance and transmittance changes in predictable directions [17]. These wavelength specific absorption and scattering produces potentially diagnostic optical patterns of vegetation conditions in deserts. A number of analytical methods have been developed for directly estimating biochemical composition and structural characteristics. An extensive review of the literature and available optical models are available online at (http://www.multimania.com/opticleaf/).

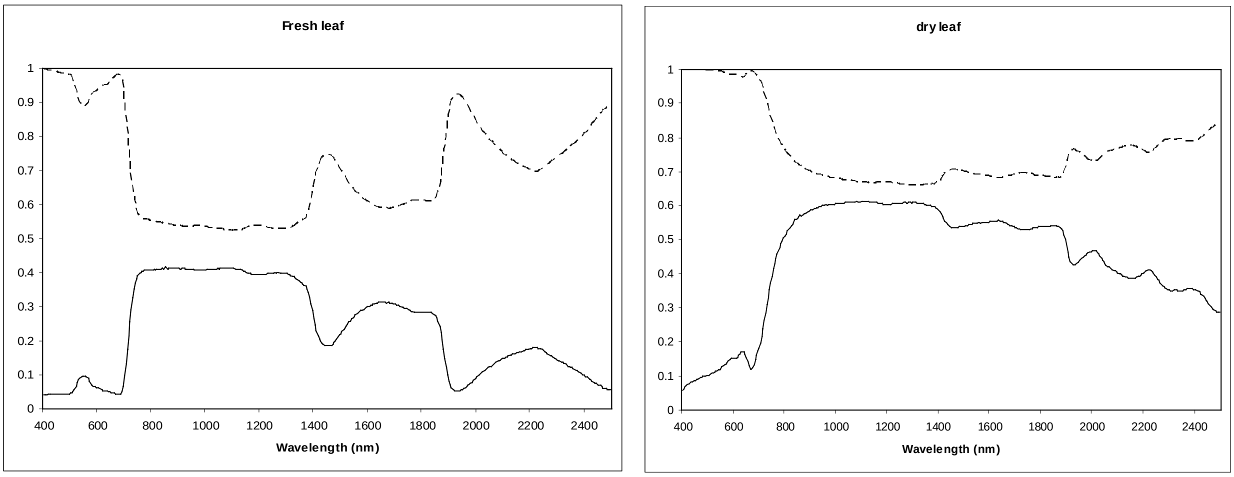

Figure 3. Reflectance (solid line) and transmittance (dashed line) of (left) fresh leaf and (right) dry leaf of a semiarid species, *Quercus pubescens*. Note that the leaf in Figure 3b was dried rapidly since strong chlorophyll absorption and red-edge features remain in the 400-700 nm region.

There is strong interest today in developing techniques to detect and quantify individual pigments [18]. The absorption of light by photosynthetic pigments dominates green leaf properties [19] in the visible (VIS) spectrum (400 - 700 nm), with a minimum at 550 nm (Figure 4a-c). Leaf inversion models, e.g., PROSPECT [20-22] predict total pigment concentration (μg cm^{-2}), by assuming that they are entirely composed of chlorophyll a and b (Figure 4a). Characterization of *in vitro* absorption coefficients for other photosynthetic pigments, e.g., xanthophylls, anthocyanins, caroteins and even chlorophyll b could further improve leaf radiative transfer models (Figure 4b). *In vitro* absorption spectra for chlorophylls and several accessory photosynthetic pigments (e.g., carotenoids, xantophylls) are available [23]. However, the pigment spectrum shifts with the solvent used to extract them, so the *in vivo* configuration of plant pigments remains uncertain. Overlapping absorption wavelengths make identification challenging.

Carotenoids are a family of red, orange, or yellow pigments, which effectively expand the wavelength range for energy absorption by photosynthesis. In photosynthesis, the energy absorbed by carotenoids is transferred to a chlorophyll a photoreceptor. Xanthophylls, a class of carotenoids, are involved in photoregulation of light by dissipating excess absorbed energy and avoiding oxidative damage to the photocenter [24]. Under excess light conditions, violaxanthin is converted to zeaxanthin in the xanthophyll cycle, which due to its absorption characteristics, increases leaf reflectance. Gamon, Penuelas, and colleagues [25-33] have extensively investigated the use of these spectral differences to develop a normalized ratio termed the Photosynthetic Reflectance Index (PRI), that is sensitive to changing xanthophylls cycle pigments. They successfully used this method to estimate photosynthetic efficiency. Stylinski et al. [34] showed that the PRI was well correlated to photosynthetic electron transport capacity in *Quercus pubescens* exposed to long term elevated CO$_2$ enrichment. Subsequently Stylinski et al. [35] showed that the PRI could track seasonal changes in carotenoid pigments and photosynthetic activity of mature semiarid evergreen shrubs.

Anthocyanins are a class of water-soluble red pigments which are not involved in photosynthesis but occur widely in flowers, fruits and leaves. They have a single absorption peak around 529 nm. Anthocyanins may also protect the photosynthetic system from excess light and/or to deter herbivory. Anthocyanins are common in leaves and stems, although their red to purple color may be masked by chlorophylls, carotenoids, or pubescence [36-37]. Under stress (e.g., high temperatures) or during early leaf development [38] they become more visible, consequently, measurement of leaf anthocyanins may be another indicator of physiological state [39],[33].

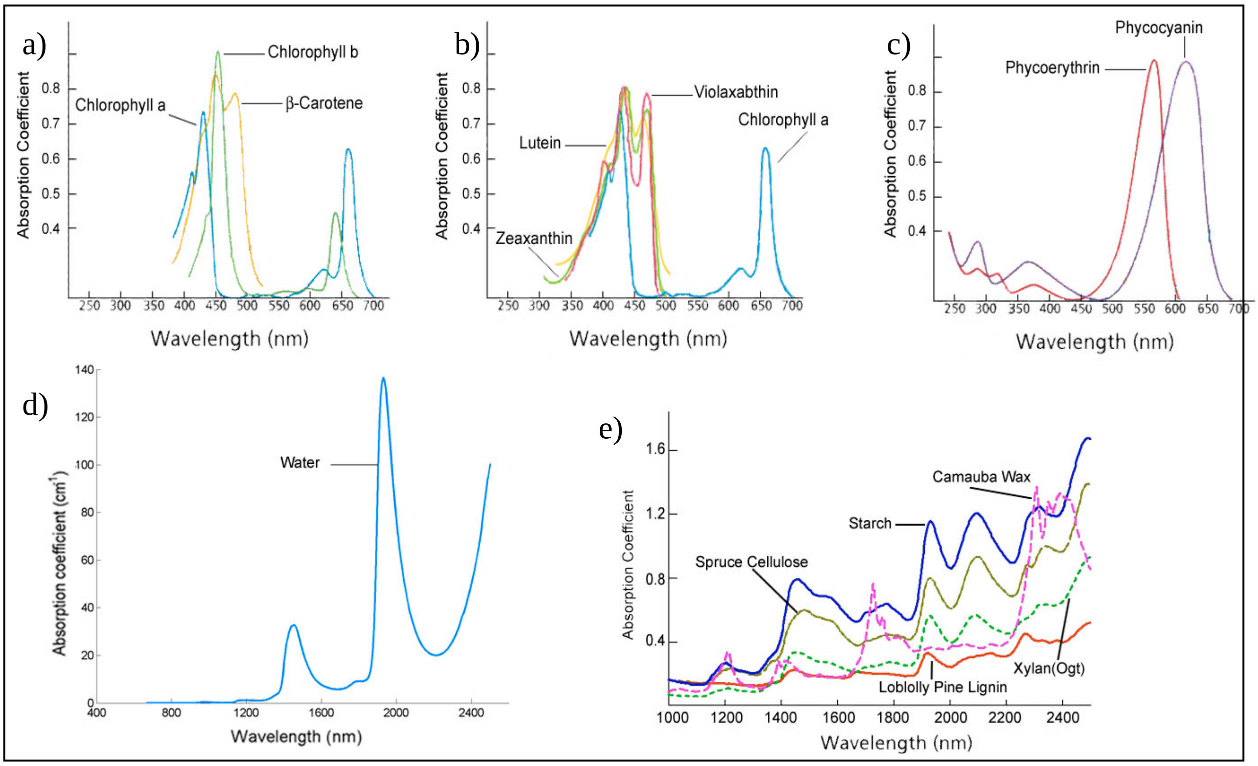

Figure 4. Specific absorption coefficients for a) chlorophyll a and b and β-carotene b) chlorophyll a and xanthopyll pigments: leutin, violaxanthin and zeathanthin, c) phycoerythrin and phycocyanin, d) water (after [40]) and e) five common biochemical compounds found in leaves.

Phycobilins, specifically phycoerytherin (red) and phycocyanin (blue) are water-soluble photosynthetic pigments that are only found in the cytoplasm of Cyanobacteria (formerly termed blue-green algae) and chloroplasts of Rhodophyta (red algae). Because cyanobacteria are the nitrogen fixing component in lichens, these are important constituents of biological soil crust. The absorption coefficients for these pigments are shown in Figure 4c which suggests that it is possible to spectrally identify and distinguish green and cynaophytic lichen classes based on pigment composition differences, if not additional lichen and algae types.

The near-infrared (NIR, 700 - 1100 nm) region has limited biochemical absorptions which are contributed by compounds characteristic of dry leaves, primarily cellulose, lignin and other structural carbohydrates. Reflectance in this region is affected by multiple scattering from internal leaf structure, including the fraction of air spaces, and refraction at air-water interfaces. As intercellular air spaces and cell sizes decrease, overall leaf reflectance or albedo declines. Eller and Willi [41]showed that pubescence acted mainly in the visible range, because in the infrared, the increase in reflectance was offset by a decrease in transmittance.

Reflectance and transmittance in the shortwave-infrared (SWIR, 1100 - 2500 nm) are dominated by water absorption in green leaves (Figure 4d). The specific absorption coefficients for pure liquid water were first observed by Curcio and Petty [42] and have been extensively studied (see [43]). The primary and secondary absorptions by water in leaf reflectance occur at 1450, 1940, and 2500 nm with important secondary absorptions at 980 nm, and 1240 nm [19]. The water absorptions result from the following vibrational modes: ν1 (H–O–H symmetric stretch mode transition), ν2 (H–O–H bending mode transition), and ν3 (H–O–H asymmetric stretch mode transition). The absorption feature at 970 nm is attributed to a 2ν1 + ν3 combination, at 1200 nm to a ν1 + ν2 + ν3 combination, at 1450 nm to a ν1 + ν3 combination, and at 1900 nm to a ν2 + ν3 combination. The fundamental water absorption is at 2800 nm.

The spectral signatures of biochemical absorptions in the SWIR region are complex. Even when substances are composed of well-characterized repeating units such as starch, sugar, and cellulose, their molecular weights vary, while others families of biochemical substances are not precisely defined or have not been isolated with their molecular structure intact (e.g., proteins, lignins). In dry leaves, reflectance and transmittance (Figure 4d,e) are controlled by dry carbon-based compounds like cellulose, lignin, and sugars, and nitrogen-based molecules such as proteins and enzymes. For example, nitrogen (N-H bonds) has a first harmonic overtone at 1510 nm and a series of combination bands at 1980, 2060, and 2180 nm [44]. Because many plant and soil macromolecules contain common chemical bonds (-H, C-N, C-O, and N-O bonds, and C=O, O=H, and N=H) they create overlapping absorption features [45-46] that have resisted specific biochemical identification.

2.2 Biophysical Information from Dry Plants

Remote sensing studies often group dry plant material as a class, termed non-photosynthetic vegetation (NPV), which is all of the non-green plant parts, including dry leaves, bark, and wood. NPV are highly spectrally variable, especially when considering a range of species [47-49]. In dry leaves, reflectance forms a more continuous monotonic spectral shape from 400 to 1500 nm. If some green foliage remains then a minor red-edge can be observed. The red-edge is a narrow spectral region between 700-725 nm at the long-wavelength edge of the chlorophyll absorption feature. It is absent in rocks, soils, and most dry plant materials. High spectral resolution studies have concentrated on identifying dry plant materials which are indistinguishable in broadband data. Baret et al. [50] showed that the position of the red-edge inflexion point was little influenced by the soil background or by the atmosphere. Elvidge et al. [51] noted that the problem in detecting trace quantities (< 10% cover) of green vegetation in arid and semiarid region could be solved by measuring the red-edge. Anecdotally, because the red-edge is considered a biosignature of green vegetation, it has become a new avenue of research for astronomers searching for life on extrasolar planets [52]!

Lignin and cellulose are usually present in plant residues in an intimate mixture, and have fundamental absorptions in the SWIR infrared, which produce several combination and overtone bands between 2000 and 2500 nm (Figure 4e). Lignin has a strong absorption in the ultraviolet at 280 nm with an absorption wing across VIS and NIR, observable after pigments have degraded in dry leaves. The combination of cellulose and lignin have two diagnostic bands around 2090 and 2300 nm (Figure 4d) which are not observable in live green vegetation [47]. Since lignin is more resistant to decay than cellulose, as plant residues decompose they become enriched in lignin and the ultraviolet absorption becomes more distinct. Thus, reflectance curves change significantly during decomposition. Nagler et al. [53] developed a Cellulose Absorption Index (CAI) using band depth at 2100 nm. Most soils do not absorb at this wavelength while plant residues do. Additionally, they found that CAI changed with soil moisture and that CAI of wet litter was significantly brighter (higher reflectance) than CAI of wet soil, and therefore, distinguishable.

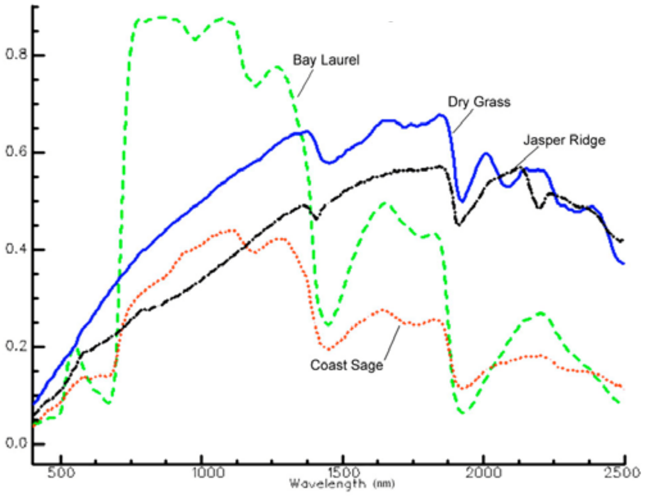

Figure 5 Typical spectra of fresh green leaf from bigberry manzanita, two stages of dry leaf weathering, and bare soil (bulano sandstone) from Jasper Ridge Biological Preserve, California, showing spectral differences that can be used to differentiate them. Note that the *Quercus pubescens* leaf in Figure 3b was dried rapidly since a strong chlorophyll absorption remains in the 400 - 700 nm region. The dry grass residue here lacks a red-edge feature.

As non-photosynthetic vegetation (NPV) decompose, significant mixing with soil occurs until eventually, cellulose decomposes and only lignin residues remain. Over time, absorption features from decomposition resistant components come to dominant the spectrum. Thus in soil, lignin features become more developed over time.

Surface residues continue to be highly variable in reflectance until decomposition progresses to the point that it becomes indistinguishable from soil [54].

One of the most complex remote sensing tasks in arid or semiarid environments is to identify NPV at various levels of cover and decomposition. When working with image data the soil background is critical to detecting variable amounts of NPV. At low NPV, the soil is the main contributor to temporal and spatial variability. While soil and NPV have a similar magnitude and spectral shape over the visible-NIR region (Figure 5), residues have narrow-band absorptions at some wavelengths, making them sufficiently distinct that they can be discriminated from soils. Wanjura and Bilbro [55] found that residue reflectance increased from 400 to 1300 nm, and decreased sharply at longer wavelengths while soil reflectance continued to increase to 1750 nm and then decreased slowly at longer wavelengths. Aase and Tanaka [56] found that residue reflectance was greater over wet soil than dry soil. Various methods have been successful in direct estimates of crop residues [53],[55],[57-61]. Since dry residues absorb more strongly in the SWIR than soils, multispectral residue indexes are based on the relationships at two wavelengths. McNairn and Protz [62] developed the Normalized Difference Index (NDI) but it is less sensitive in light colored and sandy soils, which reduces its value in arid and semiarid regions. Biard and Baret [58] transformed the NDI into a Soil Adjusted Corn Residue Index (SACRI) which reduced the index sensitivity to soil texture. They found a near linear relationship up to 20% crop residue cover, suggesting that this type of index could be applied in arid areas where vegetation cover is sparse and plant litter and soil are significant components of reflectance.

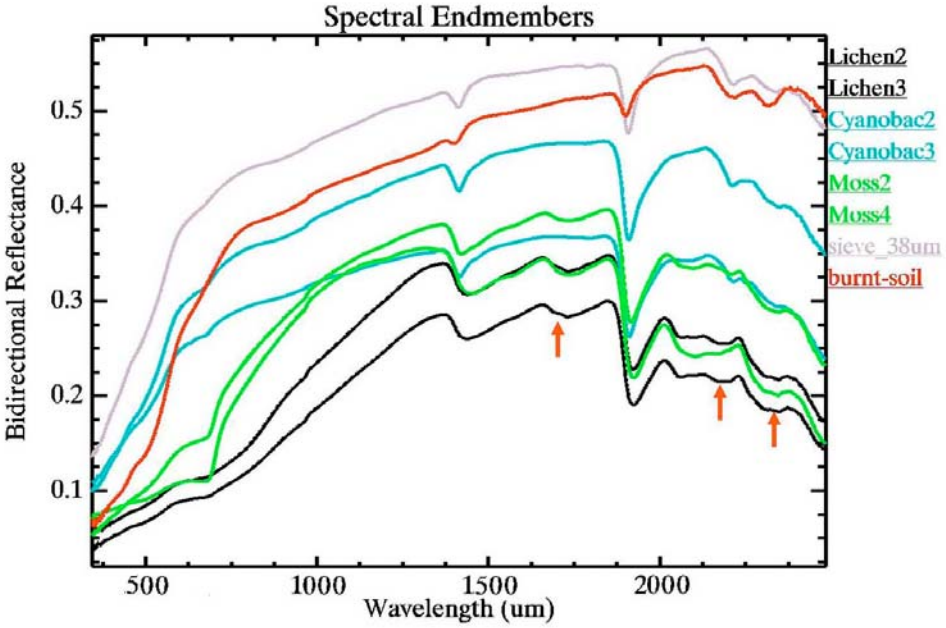

Figure 6. Components of biological soil crust from a Mojave desert habitat at the Nevada Desert Test Site, USA. Sieved and burnt (SOM exhausted) soil has higher reflectance than lichen, cyanobacteria, or mosses (P. Valco, unpublished results). Red arrows denote wavelengths where organic matter of biological curst are reported to show absorption features.

2.3 Biophysical Information from Biological Soil Crusts

Biological soil crusts (BSC) occur on every continent [63] and are a major biological component of arid ecosystems. Although they occur only the first few millimeters of the soil surface they have a key role in arid ecosystem dynamics. BSC typically account for up to 70% of the live cover in arid deserts, therefore account for much of the surface reflectance. BSC are physical and chemical associations between soil particles and microphytic mixtures of lichen, moss, fungi, cyanobacteria, and free-living algae [64-65]. BSC markedly contribute to the high spectral variability in arid regions depending on their active or dormant states and their composition (Figure 6). BSC provide critical ecological functions, including stabilizing soil, nitrogen fixation, water and nutrient retention, carbon fixation, and a seed bed for germination [63];[66-67]. BSC are typically darker than surrounding bare soil (Figure 6) thus loss increases surface albedo [68]. In contrast to BSC, abiotic physical soil crusts and chemical weathering processes are light colored, have low permeability, and are generally much thinner, often less than 1 mm. Bechtel et al. [69] and Buffoni-Hall et al. [70] showed that lichen have low transmittance, making it difficult to estimate spectral properties of the underlying rocks or soils.

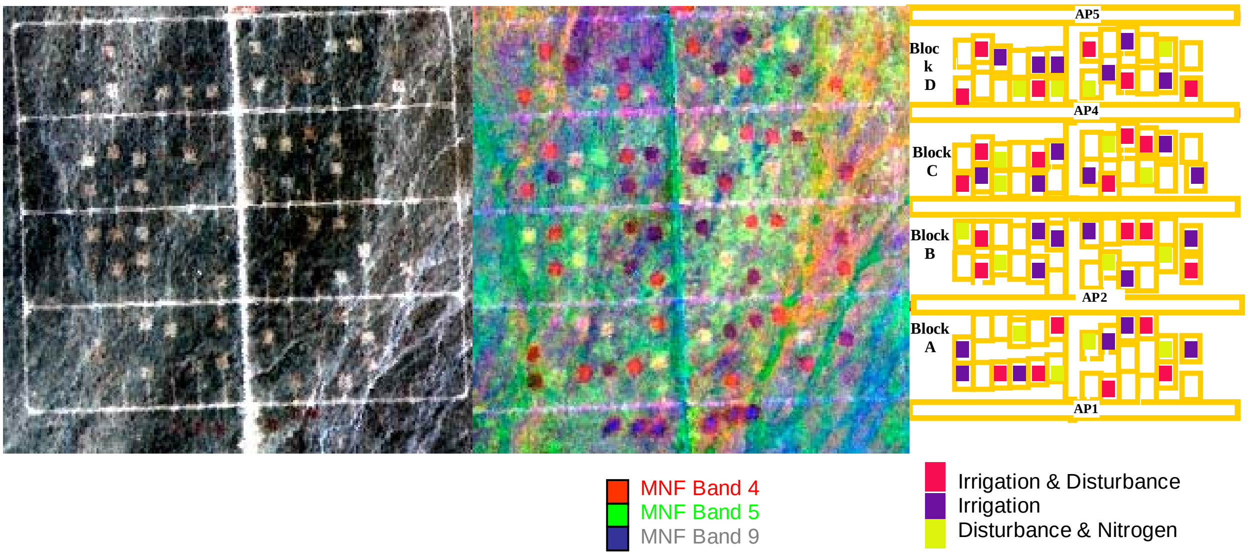

Figure 7. False color AVIRIS image (left), and minimum noise fraction image (MNF) acquired 9 July 2003 at ~3m spatial resolution over the Mojave Global Change Facility experimental plots, Nevada, USA (P. Valco, unpublished results). Each of the 96 plots is 14 m x 14 m. Treatments include added monthly summer irrigation equivalent to three extra monsoon storm events, two levels of nitrogen enrichment simulating dry deposition (added in the fall before winter precipitation period, and crust disturbance simulating effect of over-grazing, performed annually. Treatments began summer 2001.

BSC react rapidly even to low moisture inputs making their spectral responses highly variable in time. Building on Ager and Milton [71], Zhang et al. [72] used normalized spectral mixture analysis to accurately (r=0.90) separate rocks from lichen in a sub-arctic environment, a technique that might be used in arid environments. Karnieli et al. [73](1999) showed that the main spectral features were due to chlorophyll at 670 nm and organic matter at 1720, 2180, and 2309 nm (see red arrows on Figure 6). Bechtel et al. [69] used ratios of 2132/2198 nm and 2232/2198 nm to differentiate lichens from rocks. When wet, they observed NDVI as high as 0.3 comparable to vascular plants in arid regions. Rees et al. [74] used principal component analysis, and found maximum variability for arctic lichens was between 700 and 1450 nm although our data (Figure 6) show greatest variability between 1.3-2.5 µm.

Some authors suggest that BSC may be early indicators of ecosystem change because of their rapid response to environmental change [75-77]. BSC are sensitive to physical disturbance and to climate variability, including sensitivity to increased atmospheric CO_2 concentrations [68]. BSC have significantly greater lichen and moss diversity in winter rain dominated deserts than summer rain deserts with equal precipitation. The rapid wet and dry cycles that are typical of summer precipitation regimes generally increase net carbon losses and produce negligible nitrogen fixation [76-77]. Lange et al. [78] reports that CO_2 fixation in the cyanolichen, *Collema tenax* is negatively impacted by extremes of both hydration and desiccation. It is likely that increased temperatures will reduce lichen cover with secondary effects on decreased soil stability, decreased soil nitrogen, and decreased soil carbon.

The unique assemblages of biota associated with BSC create detectable spectral characteristics (Figure 6) [73-74], [79-83]. Figure 7 shows spectral changes in a Mojave desert scrub (*Larrea tridentata*, *Ambrosia dumosa*, and *Lycium* spp.) ecosystem in southern Nevada, after four years of treatments a long-term manipulation experiment. The Mojave Global Change Facility (MGCF) experiment is designed to test the cumulative and interactive effects of increased summer precipitation, increased nitrogen deposition, and increased mechanical disturbance from grazing began in 2001. (http://www.unlv.edu/climate_change_research)

2.4 Soil structural crust

In contrast to BSC, soil structural or physical crust is a thin layer (1 mm) formed by kinetic energy of drop impact over bare soils during rainstorms. The rainfall drops on the bare soil rearranges a thin surface layer by physical disintegration of the soil particles and dispersion of soil clays which migrate with water in the first few mm of soil. As a result of crust formation, infiltration decreases markedly and runoff and erosion is accentuated [84-85]. Studies show that effects are directly related to the rainfall energy so this is an important degradation process in arid regions where severe storm events bring the most precipitation and soils have a low vegetation cover. In contrast to BSC and desert varnish formation, crust formation is fast and highly dynamic, happening nearly instantaneously after a storm.

Soil crusts alter reflectance because of increased albedo, due to smaller particle size distribution [86-88], orientation of the particles [89], and enhancement of the 2200 nm absorption band by sorting montmorillonite and illite clays onto the surface. Generally there is no significant change in the carbonate 2330 nm band, because it becomes concentrated in the silt or sand fractions. Since soil crust contains higher clay content than the bulk soil, it can bias soil classifications [85]. Albedo and absorptions at 1833 and 2143 nm (no specific absorption feature) have the best correlation with raindrop energy and infiltration rate, indicating that scattering processes govern these effects [85];[90] with different soils (clay vs. sandy) producing different spectral behaviors [91]. Goldshleger et al. [91] tracked crust formation using reflectance at 1700 nm as an indicator of albedo and the first derivative of absorption at 2200 nm, which represented absorption of clay minerals. They found that a clay-particle relationship was a better indicator than particle size alone.

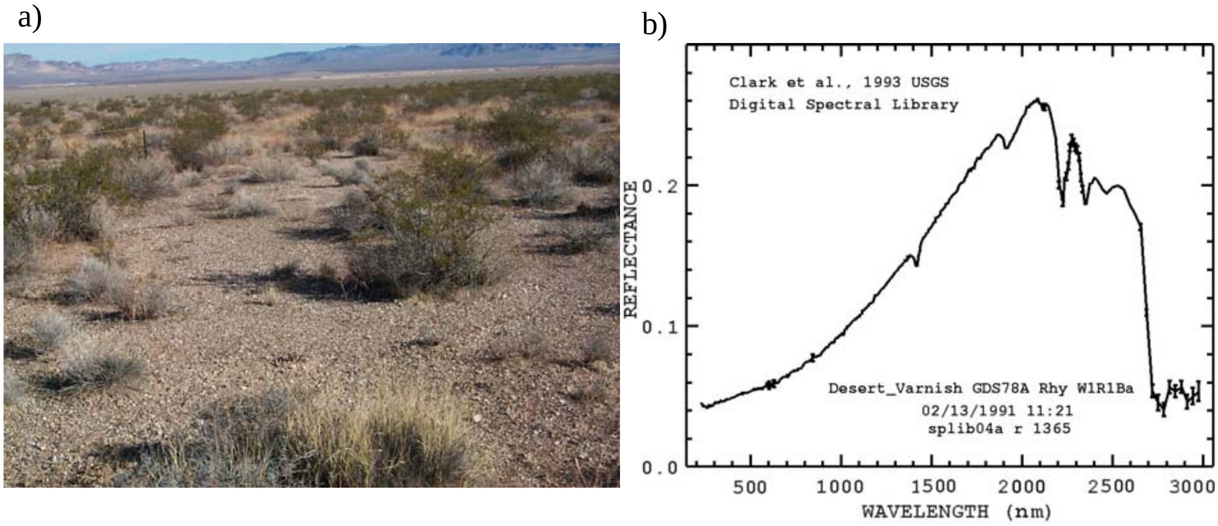

Figure 8. a) Desert pavement in Mojave Global Change Facility site, near Mercury, Nevada, USA. **b)** Spectrum of coating on desert pavement composed of rhyolite and quartz cobbles (desert varnish.gds78A) http://speclab.cr.usgs.gov.

2.5 Desert Pavement and Varnish

Although little studied for their spectral characteristics, desert pavements are important for controlling erosion and ecosystem stability and represent an early stage of biologic weathering in arid landscapes. Desert pavements (Figure 8) are ancient mosaics of rock fragments embedded in sediments [92] that occur on a wide range of undisturbed arid and semiarid landforms. The presence of desert pavement indicates that an area has been undisturbed for an extended geologic time (10,000s of years) [93]. Generally, as pavement ages the rock surfaces become smoother with few protruding fragments. Exposed surfaces are coated with thicker varnishes, which are black or brown coatings formed by bacteria interacting with clay minerals (~70%) and iron or manganese oxides [93-95]. Spectrally, desert pavement and varnish lower surface albedo relative to younger soil and rock surfaces. Loss of the pavement increases albedo by exposing native fine materials, gravel and cobbles. Disturbance may be turn over pavement and expose less weathered (oxidized) rocks of different colors, or which have a different mineralogy (less clay and manganese for example). Varnish can be mechanically removed by wind and scraping or water erosion, exposing the less weathered gravel surfaces.

2.6 Biophysical Information from Soils

The weathering process that soils undergo in arid and semiarid regions are related primarily to high temperatures and low and/or irregular availability of water. Thus, salt dissolution combined with high evaporation can precipitate alkaline salts to form hardpans and caliche layers at the wetting front. Important soil surface processes are due to the combination of irregular precipitation events, shallow soil development, and scarce vegetative cover which create low infiltration capacity and high runoff. Sparse vegetation produce little organic matter with high spatial heterogeneity. Biological and structural soil crusts have very different properties in terms of soil health and spectral properties. The combination of all these processes produces highly heterogeneous soils, which requires synoptic coverage over large regions with sufficient spatial and spectral resolution to quantify soil patterns.

Soil has less spectral structure than decomposing dry plant material (Figure 9). Since it is composed of well mixed minerals and organic matter, absorption features result from overlapping bands with no strong narrow-band absorption features such as those found in pure minerals. Consequently, soil spectra vary slowly with time [54]. The VIS and NIR reflectance is driven by a wide absorption wing that extends from the ultraviolet, due to electronic transitions of metals, mainly iron. In contrast, the general shape and specific absorption bands of the SWIR are mainly driven by water and minerals that contain water and hydroxyl ions.

Many soils only differ in brightness in red and NIR, which form a linear relationship that is represented in spectral space as a soil brightness vector [96]. The position of a given soil on the soil line depends on factors that affect the albedo such as shadows, moisture content, and roughness [97-98]. The slope of the line depends on the relative position between the R and NIR bands and therefore depends on the intrinsic soil properties such as iron or organic matter content. Also it can be affected by atmosphere and sensor properties such that it becomes soil and scene-dependent.

The width of the soil line expresses variable soil properties in these wavelengths (e.g., moisture or organic matter). To identify the source of the variability and quantify this information requires measuring additional bands. The soil line has been used to estimate vegetation cover by measuring the reflectance of a surface that is perpendicular to a soil line defined by bare soil pixels. The problem in using this index in arid environments is that the high soil heterogeneity makes it difficult to define a unique soil line. To overcome this limitation Fox et al [99]. proposed an automated soil line identification routine. The soil line only represents a two dimensional spectral space so it only shows the general shape of the spectrum in the VIS-NIR space. Most soil biological and physicochemical properties have information contained in a large number of other wavelengths that make it necessary to use more complex methodologies to study soil properties.

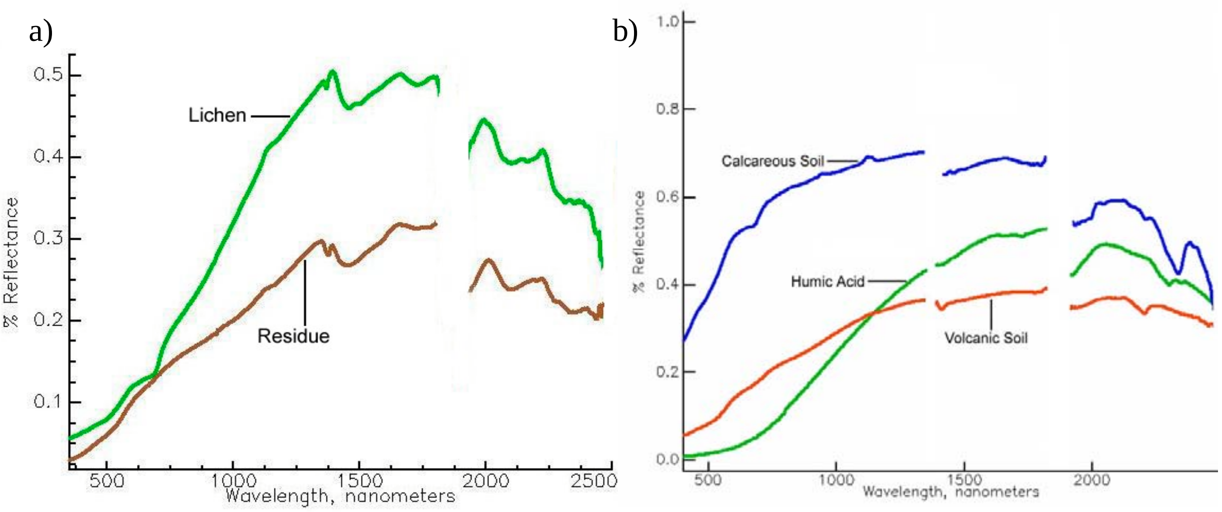

Figure 9. a) Contrasting spectral shapes between biologically active lichen and dry plant residues. **b**) Respiration resistant humic acid soil component and two contrasting soils derived from calcareous and volcanic parent material.

The most widely used semi-analytical technique to determine mineral absorption strength is the continuum removal [100-101]. The continuum removal calculates the normalized band depths by interpolating reflectance between two local reflectance maxima (the shoulders of the absorption feature) then calculates the band depth, area, and asymmetry within the wavelength interval. The mineral type is determined by the wavelength positions at the minima and the feature asymmetry [101]. However other studies [102] have demonstrated that spectral shape resulted from all interactions affecting absorption and scattering. For example, Whiting et al. [103]found water broadened and shifted the wavelength positions of specific absorption features to longer wavelengths. These changes make correlating a particular wavelength with a particular mineral chemistry and absorption depth inconsistent.

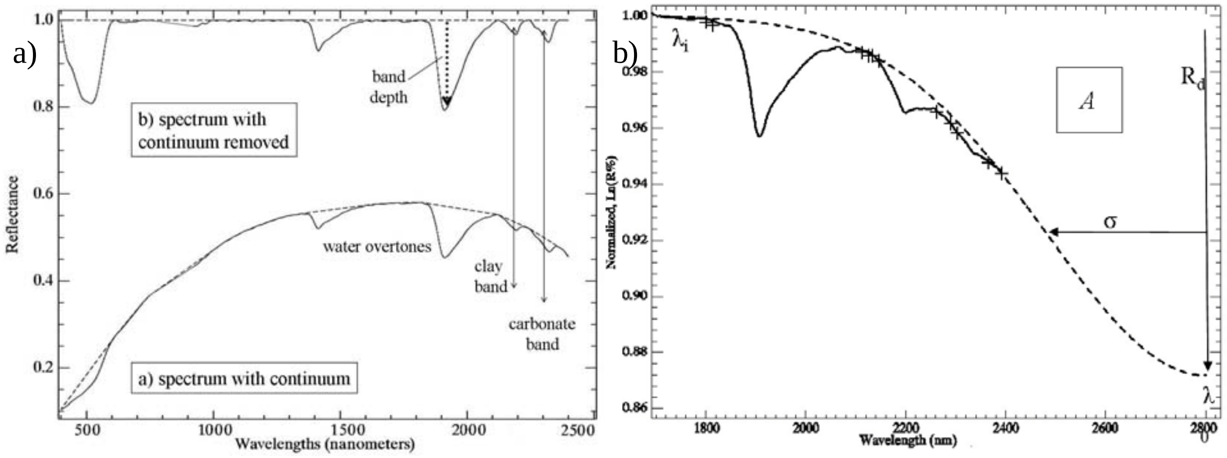

Figure 10. a) Upper, soil spectrum with continuum removed, normalizing absorption features. Lower, soil reflectance spectrum with continuum shown as dashed line. **b**) Soil Moisture Gaussian Model, fit to a soil spectrum from water fundamental at 2800 nm. The shoulders of the absorption features used for continuum removal are shown as crosses [104]. The Gaussian curve is fit from the wavelength (λ) absorption maximum to λ_i, R_d is depth at λ, σ is the full width half max, and *A* is the area.

The most complex analytical task is to distinguish bare soils and dry residues at various levels of cover and decomposition (Figures 5-9). The soil background is the main contributor to variable surface reflectance in areas with variable and/or low amounts of residue. Wanjura and Bilbro [55] found that residue reflectance increased with wavelength to 1300 nm, then it decreased sharply, while soil reflectance continued to increase to 1750 nm, and then decreased slowly at longer wavelengths (Figures 5, 9). Aase and Tanaka [56] observed that variable soil moisture looked similar to different amounts of straw on dark soil as the effect of moisture was to lower albedo across the SWIR.

Moisture is the main source of temporal variability in soil reflectance. Soil reflectance is greatly affected by slight differences in water content [105], reducing the spectral contrast needed for identifying minerals and organic matter absorption depths [106]. The change in band depth is non-linear with water content [107], which requires knowing the light absorption characteristics of the soil for all pixels in an image. Several researchers have successfully modeled soil moisture using 1450 and 1900 nm bands [107-109]. Unfortunately, these absorption bands also absorb water vapor in the atmosphere, confounding soil quantification in image data. Whiting et al. [104] extrapolated the general shape of the SWIR spectrum to the fundamental water absorption at 2800 nm by fitting the convex hull to a Gaussian function and reported that the area under the Gaussian curve is correlated with soil moisture content (r^2=0.90). The Soil Moisture Gaussian Model (SMGM) was highly correlated to the soil water content, up to the water holding capacity of the soil without dependence on specific water absorption bands.

Organic matter is closely related to soil quality and degradation processes in natural vegetation and agricultural lands. It is not only an indicator of soil degradation, but also regulating other biogeochemical processes. Aranda and Oyonarte [110] found lowest quality soil organic matter under degraded shrubs suggesting that degraded vegetation may lead to soil degradation. Both low content of OM and poor quality are characteristic of arid and semiarid environments. Organic matter has been studied by Henderson et al. [111] and Coleman and Montgomery [112] with the main effect observed in the VIS-NIR, causing high albedo and a convex hull shape for soils with low organic matter content [113]. Figure 11a shows three soils with high, low and intermediate amounts of organic matter. Demattê et al. [114] observed a decrease in reflectance between 600 and 2500 nm when organic matter content increased after applying an organic fertilizer. Chen et al. [115] mapped organic matter at the field scale using aerial photography, obtaining high accuracy in bare soil. However this task becomes more complicated in natural areas with variable vegetation, high soil variability, and low organic matter in arid areas.

Soil salinity is one of the main consequences of soil degradation. Salinization not only affects the growth of vegetation, but destruction of soil structure due to clay dispersion and subsequent decrease in infiltration and aeration. Reflectance of saline soils results from the spectral properties of salt and surface roughness, presence of crust, soil color and moisture, which have a combined effect on albedo [116]. A good review of spectral characteristics of soil salinity is found in Metternicht and Zinck [116]. Most soil salts (i.e., halite, calcium carbonate, sodium sulfate and gypsum) are highly reflective in the VIS-NIR and show distinct absorption features in the SWIR. Hydrated salts like gypsum have a significant decrease in reflectance toward longer wavelengths and sharp absorptions at the water bands, while salts like halite are highly reflective in this region of the spectrum. As a result most saline areas have high albedo except highly alkaline soils which are dark black due to distillation of organic matter. Roughness and moisture are the two factors affecting albedo. For example the presence of saline crust decreases roughness and increases albedo, while moisture dissolves salt crusts so albedo decreases. Since these properties are highly dynamic their variability makes assessment difficult. While high salt concentrations are easily identifiable, low levels present more difficulty for detection because spectral features are weak and the presence of salt-tolerant vegetation dominates the soil signal. Hypersaline soils have little or no vegetation on them but may have BSC if moisture is available.

Roughness is the primary factor affecting soil reflectance and it is also highly variable in arid soils. Surface roughness is influenced by the size and distribution of soil aggregates and by the density and distribution of any vegetation cover. The effect of roughness on albedo is on the distribution of shadows [117], which affect the spectral contrast and reduce discrimination of spectral features. However, several studies have demonstrated that bi-directional reflectance distribution is distinct on desert surfaces [118]. Thus, Shosany et al. [119] demonstrated that most soils in the Australian desert were anisotropic with a dominant backscattering component. Cierniewski and Karnielli [120] simulated reflectance on four virtual surfaces (desert pavement, BSC, sands and playa) under different illumination conditions and showed that forward scattering and backscattering properties significantly affected spectral contrasts between surfaces. For example, contrast between sand and playa was greatest in the backscattering directions for a specific view and zenith angles, while for crust and desert pavement, the contrast was best in the forward scattering direction.

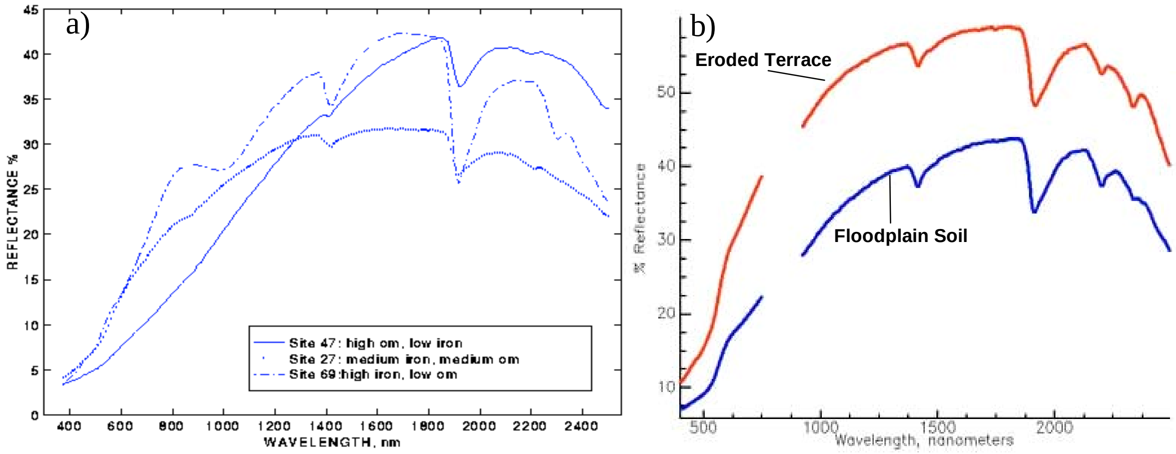

Figure 11a. Three soils showing effect of organic matter on soil reflectance. **11b.** Soil spectral from an eroded calcareous terrace and an alluvial floodplain.

Erosion is important in arid regions. Common indicators of erosion are a decrease of organic matter, appearance of lower soil horizons at the surface, and presence of rocks. Eroded soil surfaces can have high levels of iron oxides or carbonates from the B or even C horizon. Whiting et al. [103] mapped carbonates in the Tomelloso area of Spain where the underlying carbonate layer (caliche) was exposed on the surface. Figure 11b shows the spectral soil signature from the surface soil samples of an eroded terrace and from a floodplain. The eroded soil has high albedo and a strong carbonate absorption feature, while the floodplain soil has stronger clay absorption. De Jong [86] used imaging spectroscopy to map erosion based on iron and carbonates and Palacios-Orueta et al. [121] used Foreground and Background analysis on AVIRIS data to map organic matter and iron. In a spatial context, eroded soils can occupy broad extensions or form linear features like gullies or rills which are difficult to identify without high spatial resolution. Metternich and Fermont [122] mapped regional patterns of soil surface erosion using spectral mixture analysis on Landsat data.

As with spectral features of plants, any overlapping biogeochemical absorption will contribute to the total absorption causing interpretation errors [123]. Whiting et al. [124] found that classical continuum removal underestimated the band depth of carbonate and clay absorptions if the effect of adjacent mineral absorptions and water on soil reflectance was not quantified. Given the hydrophilic nature of clays, their model provided a robust methodology that could be used to obtain quantitative estimates of soil minerals. The overlapping adjacent absorption features affect reflectance along the shoulders between the absorptions [123], [125-126], lowering reflectance reducing the apparent depth of the absorption. This error in band depth significantly reduces the correlation between measured and predicted mineral content as moisture and other minerals increase. The short wavelength side of the clay absorption band at 2200 nm is affected by broadening of the water overtone at 1900 nm and an absorption at 2100 nm by dry plant material [103]. Quantifying soil moisture and adjacent allows a correct interpretation of clay and carbonate band depths. Including this model in materials that have overlapping absorption features should improve their quantification.

3 MAPPING PLANT AND SOIL PROPERTIES USING BIOPHYSIOLOGICAL INDEXES

A wide range of spectral indexes have been developed that take advantage of specific absorption features of plants and soils relative to spectral bands where the materials do not absorb [127]. These methods are quasi-quantitative in that specific chemicals absorb energy at specific wavelengths, thus we know *a priori* where these features occur. However, the absorption depth is not linear with concentration and the presence of other materials with overlapping absorption features will confound quantification. Some plant and soil chemicals of interest are actually a family of related molecules (e.g., organic matter) rather than a specific molecule (e.g., H_2O) which results in inconsistent identification of the wavelength location of absorption features, thus limiting index methods.

Vegetation indexes are sensitive to vegetation cover and provide an estimate of the “greenness” of an area. Newer indexes identify specific pigments, water content, cellulose, lignin, and nitrogen. Tables 1 and 3 list 36 widely used indexes of four basic types: pigment, foliar water, foliar chemistry, (Table I) and soil indexes (Table 3). Not all of these indexes are independent. Obviously the multiple indexes estimating chlorophyll content will be correlated. Additionally, correlations between physiological characteristics lead to further correlations between indexes. For example, the water indexes and nitrogen index are highly correlated to NDVI. This is because nitrogen increases with water as does photosynthetic machinery, resulting in higher NDVI. Conditions where indexes become uncorrelated or partially uncorrelated may provide evidence for stress conditions.

3.1 Vegetation indexes

Vegetation indexes (VI) take advantage of the strong contrast between red and NIR reflectance produced by green foliage (related to vigor and amount of vegetation). In desert environments, VIs must be able to discriminate vegetation at low cover, from zero up to about 50%, and to extract information about vegetation properties, while minimizing soil, atmosphere, and sun and view angle effects. In arid environments soil is the most significant contribution to scene variance therefore, a correction for soil background effects is necessary.

3.2 Pigment indexes

Pigment indexes focus on photosynthetic pigments, primarily chlorophyll, the dominant photosynthetic pigment of green vegetation. However, some like the PRI identify xanthophylls cycle pigments, which are important in regulating light absorption in high light intensity environments. Leaves possess a range of accessory photosynthetic pigments, including carotenoids and xanthophylls that serve functions to regulate and increase photosynthetic performance.

3.3 Foliar water indexes

Water absorbs strongly throughout the SWIR wavelengths [19]. Most narrow-band indexes use the 970 or 1240 nm water absorption features, although broad band indexes have been used (e.g., Landsat bands 4, 5 and 7).

3.4 Foliar chemistry indexes

Several leaf chemistry indexes have been proposed. The normalized difference nitrogen index (NDNI) was successfully used by Serrano et al. [128] on AVIRIS data to estimate nitrogen concentration in a semiarid shrubland. Nonetheless, other studies have found it difficult to extract this data from two band indexes. Pinzon et al. [129](1998) used singular value decomposition to accurately estimate leaf nitrogen from leaf samples in laboratory data. Later, Smith et al. [130] (2002) used partial least squares to relate field measured leaf nitrogen to canopy nitrogen in AVIRIS hyperspectral data. The cellulose absorbance index (CAI; [53]), estimates the cellulose content of senescent plant matter, emphasizing the distinctions between soil and plant litter. This index may be useful in arid and semi-arid regions where green vegetation is seasonally sparse and much of the biomass is in undecomposed plant litter and stems.

3.5 Soil indexes

To observe desert conditions and desertification it is critical to map soils with none or low amounts of vegetation. The soil line, related to soil brightness in red and NIR bands, has already been introduced. Although soil spectra lack strong absorption bands, several soil indexes (Table 3) related to soil color have been developed [131-132]. The latter found high correlation between the Helmholtz definition of color and Thematic Mapper indexes in an arid environment. Redness indexes are important for characterizing soil weathering and oxidation. Color is important for assessing soil quality and is closely related to surface processes and types of chemical weathering. Soil color is defined by parent material, weathering, and topography which are related to soil biophysical properties, therefore, color might be used as an indicator of erosion or deposition or as an indicator of surface organic matter. If soil variability is high, as in many desert environments, there will not be a unique soil line and the width of the soil line becomes critical for defining soil properties.

4 LEAF REFLECTANCE AND TRANSMITTANCE MODELS

Over the past decade, sophisticated radiative transfer models have been developed to account for leaf properties and changes in reflectance/transmittance due to changing leaf biochemistry and structure. The simplest models consider the leaf as a single scattering and absorbing plane-parallel layer while the most complicated models consider the full three-dimensional structure and biochemistry of the cells and tissues that form the leaf. At a minimum, physically realistic models require information about the refractive index and the specific absorption coefficients of leaf constituents (Figure 4). Computer-based leaf models can be categorized into different classes, arranged in order of increasing complexity (Figure 12).

4.1 Plate models

Figure 12a: Allen et al. [133] were the first to represent a compact leaf as an absorbing plate with rough surfaces producing diffusion. This approach was extended to non-compact leaves by regarding them as layers of plates separated by N–1 air spaces [134]. The parameter N provides an internal structure for scattering. The widely used PROSPECT model (Leaf Optical Properties Spectra) [20] was designed to accurately simulate the hemispherical reflectance and transmittance of various types of plant leaves (fresh monocot and dicot leaves, senescent and dry leaves) over the solar spectrum from 400 to 2500 nm. The original model was improved significantly by optimization of input parameters [21-22]; [135-137]. Its four input parameters today are the leaf structure parameter, chlorophyll a+b concentration, equivalent water thickness, and dry matter content. Recent studies [138-139] have quantified the contribution of these parameters to the PROSPECT model outputs, as well as their interactions (Figure 13), demonstrating that most foliar absorptions are accounted for in the current model, with the gray line the sum of these contributions. Clearly there is potential to improve the model in both the VIS and SWIR regions.

Table I. Vegetation Indexes Developed as Biophysical Indicators.

Index[a]	Formula	Details	Source[b]
Pigment			
SR	R_{NIR}/R_R	Index of green vegetation cover. Wavelengths, depending on sensor, e.g., NIR=845nm, R=665nm.	1
NDVI	$(R_{NIR}-R_R)/(R_{NIR}+R_R)$	Index of green vegetation cover. Wavelengths, depending on sensor., e.g., NIR=845nm, R=665nm.	1
mNDVI	$(R_{750}-R_{705})/(R_{750}+R_{705})$	Leaf chlorophyll content	2
SGR	$\sum_{n=500}^{599} R_n$	Index of green vegetation cover.	2
PRI	$(R_{531}-R_{570})/(R_{531}+R_{570})$	Xanthophyll light response ~ photosynthetic efficiency. Sensitive to carotenoid/chlorophyll ratio	3
RGR	$(R_{600-699})/(R_{500-599})$	Anthocyanins/chlorophyll	2
NPCI	$(R_{680}-R_{430})/(R_{680}+R_{430})$	Total pigments/chlorophyll	4
SRPI	R_{430}/R_{680}	Carotenoid/chlorophyll *a* content	5
NPQI	$(R_{415}-R_{435})/(R_{415}+R_{435})$	Chlorophyll degradation, detects early stress	5
SIPI	$(R_{800}-R_{445})/(R_{800}-R_{680})$	Carotenoid/chlorophyll *a* concentrations	5
PI1	R_{695}/R_{420}	Plant stress status	5
PI2	R_{695}/R_{760}	Plant stress status	5
PI3	R_{440}/R_{690}	Vegetation health index, chlorophyll fluorescence ratios	6
PI4	R_{440}/R_{740}	Vegetation health, chlorophyll fluorescence ratios	6
Water			
NDWI	$(R_{860}-R_{1240})/(R_{860}+R_{1240})$	Leaf water content	7
WBI	R_{900}/R_{970}	Leaf water content	8
Foliar chemistry			
NDNI	$[\log(R_{1680}/R_{1510})]/[\log(1/R_{1680}R_{1510})$	Foliar nitrogen concentration	9
NDLI	$[\log(R_{1680}/R_{1754})]/[\log(1/R_{1680}R_{1754})$	Foliar lignin concentration	9
CAI	$0.5(R_{2020}+R_{2220})-R_{2100}$	Cellulose & lignin absorption features, discriminates plant litter from soils	10

[a] **SR**: Simple Ratio; **NDVI**: Normalized Difference Vegetation Index; **mNDVI**: Modified NDVI; **SGR**: Summed green reflectance; **PRI**: Photochemical Reflectance Index; **RGR**: Red/Green ratio; **NPCI**: Normalized Pigments; **CRI**: Chlorophyll Ratio Index; **SRPI**: Simple Ratio Pigment Index; **NPQI**: Normalized Phaeophytinization Index; **SIPI**: Structure Intensive Pigment Index; **PI**: Pigment Index; **NDWI**: Normalized Difference Water Index; **WBI**: Water Band Index; **NDNI**: Normalized Difference Nitrogen Index; **NDLI**: Normalized Difference Lignin Index; **CAI**: Cellulose Absorption Index. [b] 1,[140]; 2, [141]; 3, [25]; 4, [29]; 5, [142]; 6, [143]; 7,[144]; 8, [32]; 9, [128]; 10, [53]

PROSPECT provides good estimates of leaf water content (equivalent water thickness) in fresh leaves, illustrated in Table 2 using data from the LOPEX experiment [21]. Likewise estimate of dry matter from dry leaves is well predicted although the prediction of dry matter content in fresh leaves is poorly predicted. For the *Quercus pubescens* example shown in Figure 3, Table 2 provides a comparison between measured and predicted chemistry. Chuvieco et al. [145] have empirically solved this problem for wildfire risk in Mediterranean ecosystems by using multi-temporal data and combining the dry biomass estimate from the driest annual period with water content from real-time estimates. Because total ecosystem biomass changes slowly over time, this method provides better estimates than direct model inversions.

a) Plate models

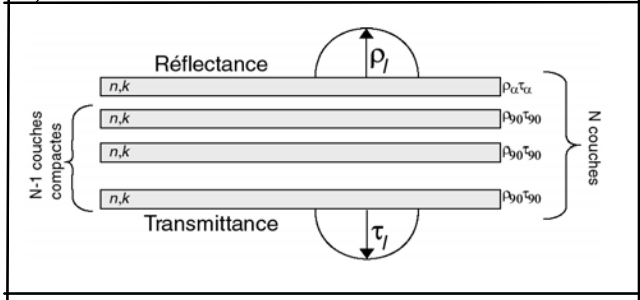

b) N-flux models

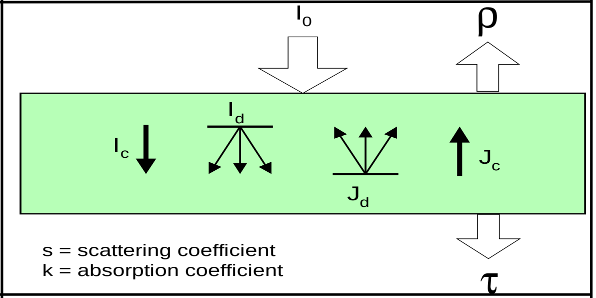

c) Compact spherical particle models

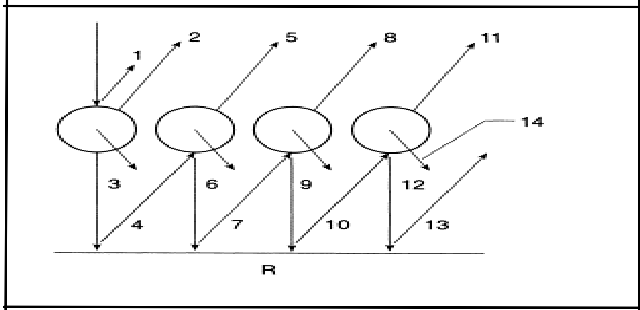

d) Radiative transfer theory

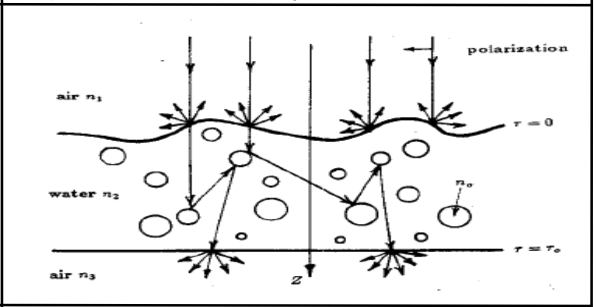

e) Stochastic models

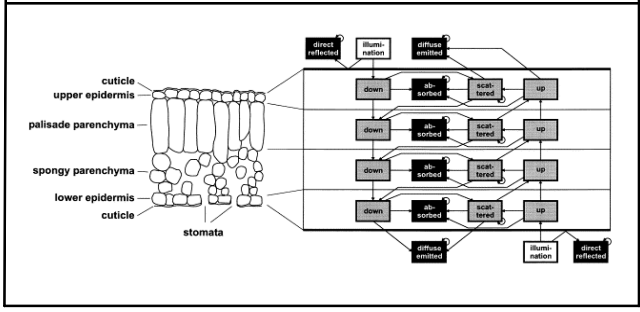

f) Ray tracing models

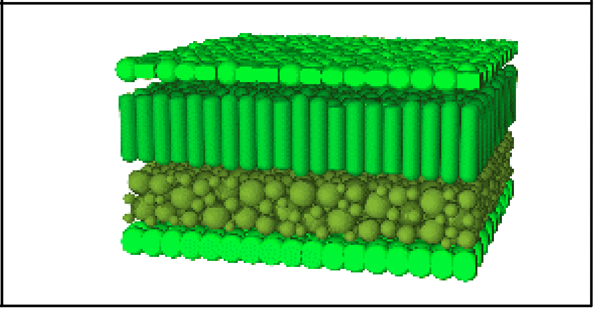

Figure 12. Major classes of models simulating leaf optical properties.

4.2 N-flux models

Figure 12b: Derived from the Kubelka-Munk theory these models consider the leaf as a slab of diffusing and absorbing materials. Different parameters are allowed in each layer and the model estimates leaf reflectance and transmittance. Leaf biochemistry was introduced by Conel et al. [146] who used a two-flux model to evaluate the influence of water, protein, cellulose, lignin, and starch on leaf reflectance, however their model was not validated.

4.3 Compact spherical particle models

Figure 12c: Dawson et al. [147] adapted Melamed's theory of light interaction with suspended powders and designed the LIBERTY model (Leaf Incorporating Biochemistry Exhibiting Reflectance and Transmittance Yields) specifically to calculate the optical properties of both dried and fresh stacked conifer (particularly pine) needles. By treating the leaf as an aggregation of cells, with multiple scattering, output reflectance and transmittance are a function of three structural parameters (cell diameter, intercellular air space, and leaf thickness) and the combined absorption coefficients for chlorophyll, water, lignin and cellulose, and nitrogen.

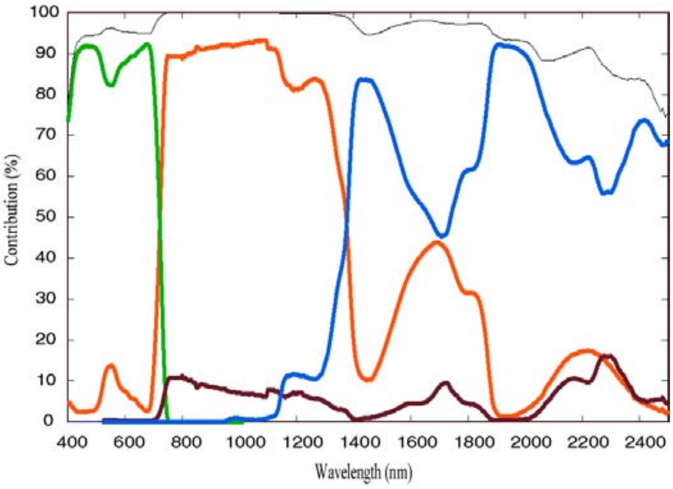

Figure 13. Contribution to leaf transmittance simulated by PROSPECT for chlorophyll concentration Cab (green), water content Cw (blue), dry matter content Cm (brown) and the structure parameter N (red) (Pavan, unpublished).

4.4 Radiative transfer equation

Figure 12d: Few leaf models directly use the radiative transfer equation because essential information about internal leaf structure and biochemical distributions is lacking, leading to major simplifications. Ma et al. [148] described the leaf as a slab of water with an irregular surface containing randomly distributed spherical particles. Ganapol et al. [149] developed LEAFMOD (Leaf Experimental Absorptivity Feasibility MODel), which models the leaf as a homogeneous mixture of biochemicals which scatter and absorb light. The homogeneity simplification ignores the obvious cellular organization of leaf chemistry. Nonetheless, Johnson[150] used this model to predict leaf nitrogen from several laboratory datasets.

4.5 Stochastic models

Figure 12e: Tucker and Garatt [151] proposed a stochastic model in which radiation transfer is simulated by a Markov chain. The leaf is partitioned into palisade parenchyma and spongy mesophyll tissues with four radiation states (solar, reflected, absorbed, and transmitted) with defined the transition probabilities. The SLOP (Stochastic model for Leaf Optical Properties) model [152] is a recent improvement in which the leaf is partitioned into four tissues.

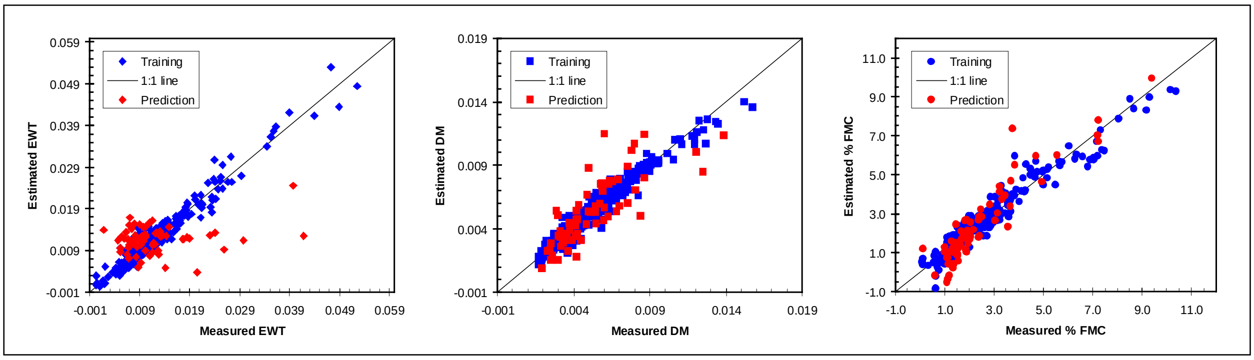

Figure 14. a) Prediction of leaf water content from fresh leaves **b)** leaf dry matter from dry leaves, and **c)** leaf dry matter from fresh leaves using a generic algorithm-partial least square regression, GA-PLS (red dots) on LOPEX leaf data for calibration and validation (blue dots). Leaf reflectance and transmission data and biochemistry from the LOPEX dataset [153]. The mean reflectance of the samples at each spectral band is subtracted before running GA-PLS.

Table 2. Leaf chemistry measured in the LOPEX dataset [21] and chemistry predictions from the PROSPECT model for an average of *five Quercus pubescens* leaf measurements.

Leaf Properties	**LOPEX Chemistry**	**Fresh Leaf Predictions**	**Dry Leaf Prediction**
N		1.38	2.97
Cab (µg/cm2)	42.7	42.2	28.1
Brown pigments (µg/cm2)	--	30.2	105.7
Cw (g/cm2)	0.00825	0.00750	0.00063
Cm (g/cm2)	0.00604	0.00604	0.00604

4.6 Ray tracing models

(Figure 12f): Only ray tracing techniques account for the full three dimensional complexity of internal leaf structure as it appears in a photomicrograph. This technique requires a detailed description of individual cells and their unique arrangement inside tissues and the optical properties of leaf materials (cell walls, cytoplasm, pigments, air cavities, etc.) must be defined. Using the laws of reflection, refraction, and absorption, the propagation of individual photons incident on the leaf surface can be simulated. Once a sufficient number of rays have been simulated, statistically valid estimates of the radiation transfer in a leaf can be predicted.

Govaerts et al. [154] used a three-dimensional ray tracing model, RAYTRAN [155], and developed a virtual three-dimensional leaf, to characterize the light environment, including absorption, scattering and transmission, within and between cells. Cells of variable size, cell wall thicknesses, chemistry, and air spaces were modeled to simulate realistic leaf tissues and the implications for absorption profiles, light harvesting, and photosynthesis was successfully investigated [156]. The model simulated the leaf anatomy of a typical mesic dorsiventral dicot leaf. In general, we lack sufficient information about leaf anatomy and biochemistry to apply this model to a wider range of morphological types, e.g., xeromorphic leaves. However, if anatomical and morphological data were available, it would be possible to simulate a range of environmental conditions and improve our understanding of biophysical measurements in arid ecosystems.

4.7 Next Generation of Leaf Models

Despite decades of research, much more work is required before we will accurately model leaf optical properties. Progress on the next generation of optical models requires improvements in understanding detailed cell and leaf anatomy for leaves having adaptations to different environmental conditions. Perhaps new approaches to modeling may lead to fundamental improvements, e.g., the ABM (Algorithmic BDF Model) or FSM (Foliar Scattering Model) which was used to study the interaction of light with plant leaves for image synthesis applications [157]. Further, more understanding of the relationships between structure and function at the leaf level are clearly needed to drive model improvements. Lastly, better optical characterization of more biochemical compounds is needed to expand the range of biochemistry that can be detected. It is not demonstrated that specific leaf photosynthetic pigments (chlorophyll a and b, carotenoids and xanthophylls) can be identified and quantified and yet this information would significantly improve understanding of the biological controls on photosynthesis. One reason for needing more information is that a direct interpretation of chlorophyll only estimates potential carbon fixation and does not measure actual state of photosynthetic activation.

A small but measurable fraction of the radiation reflected and transmitted by leaves is actually fluorescence emission [158-159] by polyphenols in the blue and chlorophyll *a* in the red and NIR as shown in Figure 15. Passive sensing of chlorophyll fluorescence in the oxygen bands emerges as a promising approach for monitoring vegetation health. However, the interpretation of this signal depends both on the leaf environment (incoming light quality and intensity, temperature, etc.) and on intrinsic parameters (physiological state, species, biochemical composition, etc.). In the FluorMOD project (Development of a Vegetation Fluorescence Canopy Model), a leaf fluorescence model has been developed that predicts reflectance and transmittance of a fresh leaf including chlorophyll fluorescence [160-161]. Beside the classical input variables for PROSPECT, fluorescence quantum yield, PSII/PSI ratio, temperature, species, and incident PAR are required. Figure 15 shows the first results of the FLUORMODLEAF for a typical dicot leaf. Although the model is still at an early stage of validation, these results are encouraging.

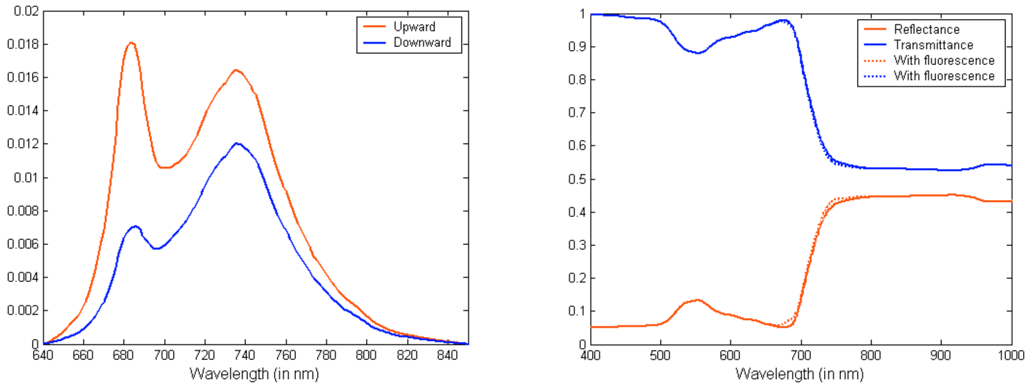

Figure 15. Simulation of the adaxial and abaxial chlorophyll fluorescence (on the left) and of the reflectance and transmittance with and without fluorescence (on the right) using FLUORMODLEAF. Structure parameter: N = 1.5, chlorophyll a+b content: C_{ab} = 33 µg cm^{-2}, equivalent water thickness: C_w = 0.025 cm, dry matter content: C_m = 0.01 g cm^{-2}, fluorescence quantum yield: Φ = 0.04, temperature: T = 20°C, species: green bean, PSII/SPI ratio: Sto = 2.0.

Many studies have demonstrated a direct relationship between photosynthetic rates, light absorbance, chlorophyll content, leaf nitrogen, and dry matter production are all related to leaf area (e.g., [26]; [162-163]. There appears to be a linear dependence of maximum photosynthetic capacity on leaf nitrogen [164] which is partially species specific. Leaf nitrogen exhibits a linear relationship with specific leaf mass, the reciprocal of specific leaf area (1/specific leaf area) [165], and a property inversely related to dry biomass estimated by PROSPECT.

As described earlier, hairy and/or waxy leaves are typical of plants in arid regions. Specific surface optical properties of these leaves are poorly known. For instance, a thick cuticle, which may protect leaves from desiccation or insects acts as a mirror, preferentially reflecting light in the specular direction. In contrast, hairs tend to scatter light in all directions. This duality between specular and Lambertian surfaces is characteristic of the leaf bidirectionnal reflectance distribution function (BRDF). Leaf BRDF was recently acquired for several species using a goniophotometer at 400 wavelengths and 98 viewing angles [166]. These measurements (Figure 16) have been successfully estimated with a specular reflection model (Cook-Torance) coupled with PROSPECT to simulate the diffuse fraction.

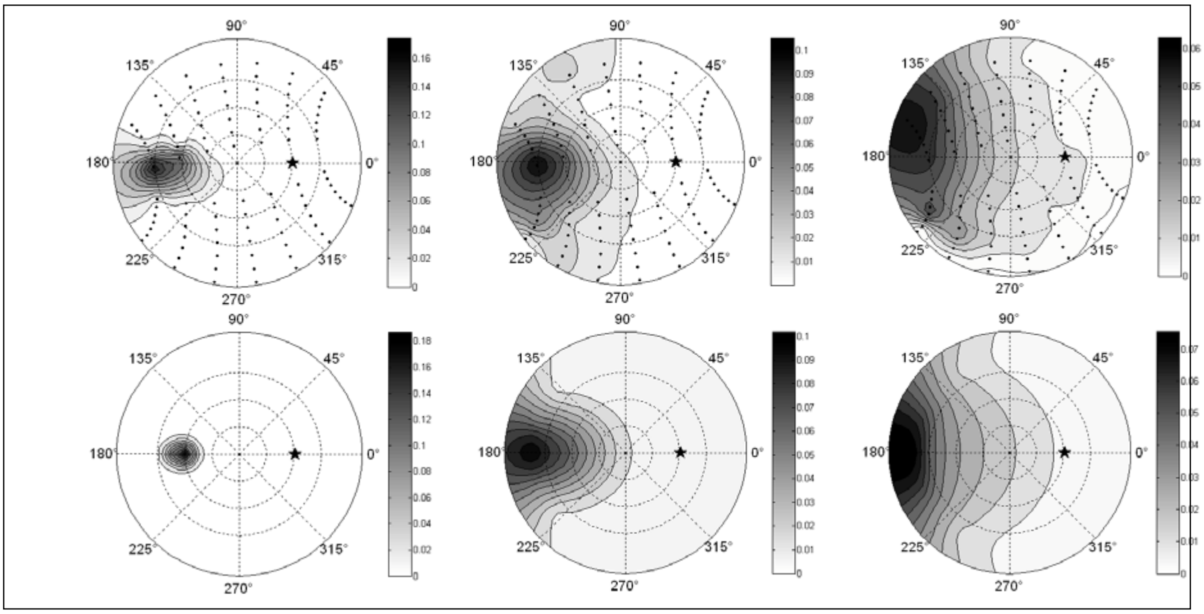

Figure 16: Measured (top) and modeled (bottom) BRDF for θ_s = 41° at wavelengths of minimum reflection (after Bousquet et al., 2005).

4.8 Extending biophysical measurements to canopy models

Heterogeneous and open plant canopies, characteristic of desert environments, preclude the use of simple 1-D radiative transfer models that rely on an assumption of homogenous turbid media [167]. On such surfaces, the interactions between light and the various objects (for instance, shrubs, grasses, BSC, bare soil), which are distributed in clumped patches rather than uniformly distributed, generate a higher level of complexity that requires 3-D models [168]. Esteve et al.[169] used the DART (Discrete Anisotropic Radiative Transfer) model [170], to simulate radiative transfer in heterogeneous arid 3-D landscape comprised of trees, shrubs, grass, soil, etc. They inverted DART on a temporal series of Landsat MSS acquired in Burkina Faso, and determined the woody cover allowing them to follow its degradation over time. Zarco-Tejada et al. [171] followed changing leaf water content over the summer drought in semiarid southern California using a MODIS time series analyzed with a linked PROSPECT and SAILH canopy model. Some information about surface heterogeneity, which may change fast when land degradation occurs, can also be inferred using multi-angular reflectance data. Widlowski et al. [172] generated various 3-D vegetation canopy representations, from homogeneous to heterogeneous, at the nominal ground resolution of the MISR instrument and simulated their reflectance using RAYTRAN. They showed that the reflectance anisotropy could be obtained by inversion of a simple parametric model.

5 SOIL REFLECTANCE MODELS

Most soil mapping has been related to the fraction of exposed soil or more precisely, the fraction of green vegetation cover, assuming that non-vegetated surfaces are soil. To date the identification of soil biogeochemical components from reflectance measurements have been largely limited to regression models that are valid only for specific locations. Greater use of multivariate statistical models, e.g., neural nets or support vector machines, will provide techniques that increase accuracy of soil quantities and portability across larger regions. Wider use of classification and regression tree (CART) models, partial least-squares, and general additive model (GAM) methods may also improve local regression models by including more spatial data in the analysis, and provide the templates for applying methods in other soil regions. These regression models may also benefit from the inclusion of hierarchical partitioning the surface reflectance components as a means of stratifying the image region to improve the local spectral model, just as much as landscape partitioning improves the accuracy.

The greater task, although highly promising for producing more robust models, is in developing radiative transfer models that can identify the presence and abundance of soil components in the context of intimate mixtures and surface geometry. Knowledge gained in recent years in extending radiative transfer modeling to a wider range of vegetation and soil backgrounds will restart soil modeling efforts begun in 1990’s. The identification of absorption coefficients for soil minerals, organic matter, and water are needed to develop radiative transfer models that will measure mineral abundance through spectral curve fitting.

6 CONCLUSION

The geographic extent and remote locations of arid ecosystems and the harsh climate characteristic of arid ecosystems create challenges to effectively monitoring desertification. Furthermore monitoring must be done over long periods to fully observe the stochastic behavior of deserts in a globally changing context. The potential to use remote sensing for cost-effective monitoring has long been recognized, although the extensive heterogeneity of geologic parent material and soils combined with low vegetative cover, rapid biologic responses to wet and dry rainfall pulses, has limited our ability to fully monitor the condition of these ecosystems. Furthermore, infrequent precipitation leads to extended dormancy with short unpredictable periods of biological activity. We reviewed the spectral characteristics of plants and soils that are detectable using optical sensors and current methods to identify and quantify properties that have potential for monitoring arid ecosystem processes. The wealth of existing information on the reflectance and transmittance of desert plants, soils, and other materials, combined with new modeling and index approaches will lead to improved capability for monitoring global desert environments.

A wide range of plant biochemicals are detectable or potentially detectable in hyperspectral data, e.g., chlorophyll, photosynthetic accessory pigments, water, and soil constituents e.g., clays, carbonate, iron, and organic matter. Biophysical methods may improve detection and monitoring of inter-plant spaces composed of bare soil crust, biological soil crust, or dead plant material. The expanded use of absorption features in the VIS and SWIR has produced a large number of spectral index-based methods to identify specific compounds or properties. As we move toward more quantitative predictive models, it is clear that the overlapping structure of many absorption features of plants and soils precludes direct assessment of their concentration. New biophysical methods that take the full spectral shape into account, including the effect of one compound on the spectral absorption of another, are needed to reduce uncertainty in their estimates. Over the past decade several radiative transfer models have been developed based on physical absorption and scattering processes using principles of spectroscopy and information over the entire spectrum. Other models take advantage of new types of data like passive fluorescence or thermal-infrared emissions or bidirectional reflectance.

Table 3. Soil Indexes Developed as Biophysical Indicators.

Index[a]	Formula	Details	Source[b]
NDI	$(R_{840}-R_{1650})/(R_{840}+R_{1650})$	Discriminates soil and dry matter	1
SACRI	$\dfrac{\alpha(R_{840}-\alpha R_{1650}-\beta)}{R_{1650}-\alpha R_{840}-\alpha\beta}$	Improved NDI discrimination	2
CRIM			3
	TM Indices	**HRV Indices**	
BI	$BI=\sqrt{(TM1^2+TM2^2+TM3^2)/3}$	$BI=\sqrt{(XS1^2+XS2^2)/2}$	4
SI	$SI=(TM3-TM1)/(TM3+TM1)$		5
HI	$HI=(2\times TM3-TM2-TM1)/(TM2-TM1)$		5
CI	$CI=(TM3-TM2)/(TM3+TM2)$	$CI=(XS2-XS1)/(XS2+XS1)$	6, 7
RI	$RI=TM3^2/(TM1\times TM2)$	$RI=XS2^2/XS1^3$	7
RI		$RI=XS2^2/XS1^4$	4

[a] **NDI**: Normalized Index; **SACRI**: Soil Adjusted Crop Residue Index; **CRIM**: Crop Residue Index Multiband; **BI**: Brightness Index -average soil reflectance; **SI**: Saturation Index-spectral slope; **HI**: Hue Index- dominant wavelength; **CI**: Coloration Index- hematite/ hematite+geothite ratio; **RI**: Redness Index -Hematite Content. [b] 1, [62]; 2, 3 [58]; 4, [132]; 5, [175]; 6, [176]; 7, [131].

ACKNOWLEDGEMENTS

A significant part of this review was done while the first author was on sabbatic at the Department of Geography and Environmental Sciences, University of Auckland, New Zealand. The authors wish to thank Margaret Andrew for her help in assembling the index information and references for Table I and Dr. David Riaño for help in preparing some figures. We wish to thank Van Lay for help in formatting the document and references and preparation of other figures.

REFERENCES

[1] MILLENNIUM ECOSYSTEM ASSESSMENT, 2005: Ecosystems and Human Well-Being: Desertification Synthesis, Desertification synthesis. U.N. Convention to Combat Desertification (UNCCD).

[2] MEIGS, P., 1953: World distribution of arid and semi-arid homoclimates. In: Reviews of research on arid zone hydrology. pp. 203-209. Paris, United Nations Educational, Scientific, and Cultural Organization, Arid Zone Programme-1.

[3] SCHLESINGER, W.H., REYNOLDS, J.F., CUNNINGHAM, G.L., HUENNEKE, L.F., JARRELL, W.M., VIRGINIA, R.A., AND WHITFORD, W.G., 1990: Biological Feedbacks in Global Desertification. *Scence 247*, pp. 1043-1048.

[4] OKIN, G.S., MAHOWALD, N., CHADWICK, O.A., AND ARTAXO, P., 2004: Impact of desert dust on the biogeochemistry of phosphorus in terrestrial ecosystems. *Global Biogeochem. Cy. 18*, Art. No. GB2005.

[5] SCHEFFER, M., HOLMGREN, M., BROVKIN, V., AND CLAUSSEN, M., 2005: Synergy between small- and large-scale feedbacks of vegetation on the water cycle. *Glob. Change Biol. 11*, pp. 1003-1012.

[6] BEATLEY, J.C., 1980: Fluctuations and Stability in Climax Shrub and Woodland Vegetation of the Mojave, Great Basin and Transition Deserts of Southern Nevada. *Israel J. Bot. 28*, pp. 149-168.

[7] DREGNE, H.E. 1986: Desertification of arid lands, in Physics of desertification. In: El-Baz, F. and Hassan, M.H.A., (eds.): Physics of Desertification. Dordrecht, The Netherlands: Martinus, Nijhoff.

[8] NOY-MEIR, I., 1973: Desert ecosystems: environmenta and producers. *Annu. Rev. Ecol. Syst. 4*, pp. 25-41.

[9] Reynolds, J.F., Kemp, P.R., Ogle, K., and Fernandez, R.J., 2004: Modifying the pulse-reserve" paradigm for deserts of North America: precipitation pulses, soil water, and plant responses. *Oecologia 141*, pp. 194-210.

[10] Scanlon, B.R., Levitt, D.G., Reedy, R.C., Keese, K.E., and Sully, M.J., 2005: Ecological controls on water-cycle response to climate variability in deserts. *Proc. Nat. Acad. Sci. 102*, pp. 6033-6038

[11] Beatley, J.C., 1974: Effects of rainfall and temperature on the distribution and behavior of *Larrea tridentata* (creosote-bush) in the Mojave Desert of Nevada. *Ecology 55*, pp. 245-261.

[12] Smith, S.D., Huxman, T.E., Zitzer, S.F., Charlet, T.N., Housman, D.C., Coleman, J.S., Fenstermaker, L.K., Seemann, J.R., and Nowak, R.S., 2000: Elevated CO2 increases productivity and invasive species success in an arid ecosystem. *Nature 408*, pp. 79-81.

[13] Charney, J., Quirk, W.J., Chow, S.H., and Kornfield, J., 1977: comparative-study of effects of albedo change on drought in semi-arid regions. *J. Atmos. Sci. 34*, pp. 1366-1385.

[14] Smith, S.D., Monsoon, R.K., and Anderson, J.E., 1997: Physiological Ecology of North American Desert Plants. Springer, Berlin.

[15] Ehleringer, J.R., and Björkman, O., 1978: Pubescence and leaf spectral characteristics in a desert shrub, *Encelia farinosa*. *Oecologia 36*, pp. 151-162.

[16] Ehleringer, J.R., and Mooney, H.A., 1978: Leaf hairs: effects on physiological activity and adaptive value to a desert shrub. *Oecologia 37*, pp. 183-200.

[17] Rotondi, A., Rossi, F., Asunis, C. and Cesaraccio, C., 2003: Leaf xeromorphic adaptions of some plants of a coastal Mediterranean macchia ecosystem. *J. Mediterranean Ecol. 4*, pp. 25-35.

[18] Ustin, S.L., Roberts, D.A., Gamon, J.A., Asner, G.P., and Green, R.O., 2004: Using Imaging Spectroscopy to Study Ecosystem Processes and Properties. *Bioscience 54*, pp. 523-534.

[19] Carter, G.A., 1991: Primary and secondary effects of water content on the spectral reflectance of leaves. *Am. J. Bot. 78,* pp. 916-924.

[20] Jacquemoud S., and Baret, F., 1990: PROSPECT: a model of leaf optical properties spectra. *Remote Sens. Environ. 34*, pp. 75-91.

[21] Jacquemoud S., Ustin S.L., Verdebout J., Schmuck G., Andreoli G., and Hosgood B., 1996: Estimating leaf biochemistry using the PROSPECT leaf optical properties model. *Remote Sens. Environ.56,* pp. 194-202.

[22] Jacquemoud S., Bacour C., Poilve H., and Frangi J.-P., 2000: Comparison of four radiative transfer models to simulate plant canopies reflectance–Direct and inverse mode. *Remote Sens. Environ. 74*, pp. 471-481.

[23] Lichtenthaler, H.K., 1987: Chlorophylls and carotenoids: pigments of photosynthetic biomembranes. *Methods Enzymol. 148*, pp. 350-382.

[24] Dey, P. M., and Harborne, J.B., 1997: Plant Biochemistry. Academic Press Inc.

[25] Gamon, J.A., Penuelas, J., and Field, C.B., 1992: A narrow-waveband spectral index that tracks diurnal changes in photosynthetic efficiency. *Remote Sens. Environ. 41*, pp. 35-44.

[26] Gamon J.A., Field, C.B., Roberts, D.A., Ustin, S.L., and Valentini, R., 1993: Functional patterns in an annual grassland during an AVIRIS overflight. *Remote Sens. Environ. 44*, pp. 239-253.

[27] Gamon, J.A., Serrano, L., and Surfus, J.S., 1997: The photochemical reflectance index: an optical indicator of photosynthetic radiation use efficiency across species, functional types, and nutrient levels. *Oecologia 112*, pp. 492-501.

[28] Gamon, J.A., and Qiu, H-L., 1999: Ecological applications of remote sensing at multiple scales. In: F.I. Pugnaire and F. Valladares (eds.): Handbook of Functional Plant Ecology. pp. 805-266. Marcel Dekker, Inc. New York.

[29] Penuelas, J., Baret, F., and Filella, I., 1995a: Semi-empirical indexes to assess carotenoids/chlorophyll a ratio from leaf spectral reflectance. *Photosynthetica 31*, pp. 221-230.

[30] Penuelas, J., Filella, I., and Gamon, J.A., 1995b: Assessment of photosynthetic radiation-use efficiency with spectral reflectance. *New Phytol. 131*, pp. 291-296.

[31] Penuelas, J., Filella, I., and Gamon, J.A., Field, C.B., 1997a: Assessing photosynthetic radiation-use efficiency of emergent aquatic vegetation from spectral reflectance. *Aquat. Bot. 58*, pp. 307-315.

[32] Penuelas, J., Pinol, J., Oqaya, R., and Filella, I., 1997b: Estimation of plant water concentration by the reflectance Water Index WI (R900/R970). *Int. J. Remote Sens. 18*, pp. 2869-2875.

[33] Sims, D.A. and Gamon, J.A., 1999: Estimating anthocyanin, chlorophyll, and carotenoid concentrations using hyperspectral reflectance. Poster, Ecol. Soc. Ann. Meet., 1999.

[34] Stylinski, C.D., Oechel, W.C., Gamon, J.A., Tissue, D.T., Miglietta, F., and Raschi, A., 2000: Effects of lifelong [CO2] enrichment on carboxylation and light utilization of Quercus pubescens Willd. examined with gas exchange, biochemistry and optical techniques. *Plant Cell Environ. 23*, pp. 1353-1362.

[35] Stylinski, C.D., Gamon, J.A., Oechel, W.C., 2002: Seasonal patterns of reflectance indicesindexes, carotenoid pigments and photosynthesis of evergreen chaparral species. *Oecologia 131*, pp. 366-374

[36] Neill, S. and Gould, K.S., 1999: Optical properties of leaves in relation to anthocyanin concentration and distribution. *Can. J. Bot. 77,* pp. 1777-1782.

[37] Lee, D.W., and Gould, K.S., 2002: Why leaves turn red: pigments called anthocyanins probably protect leaves from light damage by direct shielding and by scavenging free radicals. *Am. Sci. 90,* pp. 524-528.

[38] Hoch W.A., Zeldin, E.L. and McCown, B.H., 2001: Physiological significance of anthocyanins during autumnal leaf senescence. *Tree Physiol 21,* pp. 1-8.

[39] Curran, P.J., Dungan, J.L., Macler, B.A., and Plummer, S.E., 1991: The effect of a red leaf pigment on the relationship between red edge and chlorophyll concentration. *Remote Sens. Environ. 35,* pp. 69-76.

[40] Kou, L., Labrie, D., and Chylek, P., 1993: Refractive indicesindexes of water and ice in the 0.65-2.5 µm spectral range. *Appl. Opt. , 32,* pp. 3531-3540.

[41] Eller, B.M., and Willi, P., 1977: The significance of leaf pubescence for the absorption of global radiation by *Tussilago farfara L. Oecologia 29,* pp. 179-187.

[42] Curcio, J.A., and Petty, C.C., 1951: The near infrared absorption spectrum of liquid water. *J. Opt. Soc. Am. 41,* pp. 302-304.

[43] Prahl, S., 2001: Optical absorption of water. Oregon Medical Laser Center. http://omlc.ogi.edu/spectra/water/

[44] Wessman, C.A. 1990. Evaluation of canopy biochemistry. In: Hobbs R.J. and H.A. Mooney (eds.): Remote Sensing of Biosphere Functioning. pp. 135-156. Springer-Verlag, New York.

[45] Grossman, Y.L., Ustin, S.L., Sanderson, E., Jacquemoud, S., Schmuck, S. and Verdebout J., 1996: Critique of Stepwise Multiple Linear Regression for the Extraction of Leaf Biochemistry Information from Leaf Reflectance Data. *Remote Sens. Environ. 56,* pp. 182-193.

[46] Barton, F.E., II, Himmelsbach, D.S., Duckworth, J.H., And Smith, M.J., 1992: Two-dimensional vibration spectroscopy: correlation of mid- and near-infrared regions. *Appl. Spectrosc. 46,* pp. 420-429.

[47] Elvidge, C.L., 1990: Visible and NIR reflectances characteristics of dry plant materials. *Int. J. Remote Sens. 2,* pp. 1775-1795.

[48] Asner, G.P., 1998: Biophysical and biochemical sources of variability in canopy reflectance. *Remote Sens. Environ. 64,* pp. 234-253.

[49] Roberts, D.A., Ustin, S.L., Ogunjemiyo, S., Greenberg, J., Dobrowski, S.Z., Chen, J., and Hinckley, T.M., 2004: Spectral and structural measures of northwest forest vegetation at leaf to landscape scale. *Ecosystems 7,* pp. 545-562.

[50] Baret, F., Jacquemoud, S., Guyot, G. And Leprieur, C., 1992: Modeled analysis of the biophysical nature of spectral shifts and comparison with information content of broad bands. *Remote Sens. Environ. 41,* pp. 133-142

[51] Elvidge, C.D., Chen, Z.K., Groeneveld, D.P., 1993: Detection of trace quantities of green vegetation in 1990 AVIRIS data. *Remote Sens. Environ. 44,* pp. 271-279.

[52] Seager, S., Turner, E.L., Schafer, J., and Ford, E.B., 2005: Vegetation’s red edge: a possible spectroscopic biosignature of extraterrestrial plants. *Astrobiology 5,* pp. 372-390.

[53] Nagler, P.L., Daughtry, C.S.T., and Goward, S.N., 2000: Plant litter and soil reflectance. *Remote Sens. Environ. 71,* pp. 207-215.

[54] Baumgardner, M.F., Silva, L.F. Biehl, L.L., and Stoner, E.R., 1985: Reflectance properties of soils. *Adv. Agron. 38,* pp. 1-44.

[55] Wanjura, D. F. and Bilbro, J.D., 1986. Ground Cover and Weathering Effects on Reflectances of Three Crop Residues. *Agron. J. 78,* pp. 694-698.

[56] Aase, J.K., and Tanaka, D.L., 1991: Reflectances from four wheat residue cover densities as influenced by three soil backgrounds. *Agron. J. 83,* pp. 753-757.

[57] Abers, J.D., Wessman, C.A., Peterson, D.L., Melillo, J.M., and Fownes, J.H., 1990: Remote sensing of litter and soil organic matter decompsition in forest ecosystems. In: R.J. Hobbs & H.A. Mooney, (eds.): Remote Sensing of Biosphere Functioning, pp. 87-103. Springer-Verlag, New York.

[58] Biard, F. And Baret, F., 1997: Crop residue estimation using multiband reflectance. *Remote Sens. Environ.* 59, pp. 530-536.

[59] Streck, N.A., Rundquist, D., and Connot, J., 2002. Estimating residual wheat dry matter from remote sensing measurements. *Photogram. Eng and Remote Sens. 68,* p.1193-1201.

[60] Vina, A., Peters, A.J., and Ji, L. 2003: Use of multispectral ikonos imagery for discriminating between conventional and conservation agricultural tillage practices. *Photogram. Eng and Remote Sens. 69,* pp. 537-544.

[61] Whiting, M.L., DeGloria, S.D., Benson, A.S., and Wall, S.L., 1987: Estimating conservation tillage residue using aerial photography. *J. Soil Water Conserv. 42,* pp. 130-132.

[62] McNairn, H., and Protz, R. 1993: Mapping corn residue cover on agricultural fields in Oxford County, Ontario, using Thematic Mapper. *Can. J. Remote Sens. 19*, pp. 152-159.

[63] Belnap, J., Budel, B., and Lange, O.L., 2001a: Biological soil crusts: Characteristics and distribution, In: Belnap, J. and Lange, O.L. (eds.): Biological Soil Crusts: Structure, Function, and Management. pp. 3-30. Springer-Verlag, Berlin.

[64] Belnap, J., 2001a: Comparative structure of physical and biological soil crusts. In: Belnap, J. and Lange, O.L. (eds.): Biological Soil Crusts: Structure, Function, and Management. pp. 177-192. Springer-Verlag, Berlin.

[65] Belnap, J., 2001b: Biological soil crust and wind erosion. In: Belnap, J. and Lange, O.L. (eds.): Biological Soil Crusts: Structure, Function, and Management. pp. 339-348. Springer-Verlag, Berlin.

[66] Belnap, J., and Gardner, J.S., 1993: Soil microstructure in soils of the Colorado Plateau: the role of the cyanobacterium Microcoleus vaginitus. *Great Basin Naturalist 53*, pp. 40-47.

[67] Harper, K.T. and Belnap, J., 2001: The influence of biological soil crusts on mineral uptake by associated vascular plants. *J. Arid Environ. 47*, pp. 347-357.

[68] Belnap, J., and Eldridge, D.J., 2001: Disturbance and recovery of biological soil crusts. In: Belnap, J. and Lange, O.L. (eds.): Biological Soil Crusts: Structure, Function, and Management. pp. 363-384. Springer-Verlag, Berlin.

[69] Bechtel, R., Rivard, B., and Sanchez-Azfeifa, 2002: Spectral properties of foliose and crustose lichens based on laboratory experiments. *Remote Sens. Environ. 82*, pp. 389-396.

[70] Buffoni Hall, R.S., Bornman, J.F., and Björn, L.O., 2002: UV-induced changes in pigment content and light penetration in the fruticose lichen *Cladonia* arbuscula ssp. *mitis*. *J. Photochemistry and Photobiology. B, Biology 66*, pp. 13-20.

[71] Ager, C.M., and Milton, N.M., 1987: Spectral reflectance of lichens and their effects on the reflectance of rock substrates. *Geophysics*, 52:898-906.

[72] Zhang, J.K., Rivard, B., Sanchez-Azofeifa, A., 2005: Spectral unmixing of normalized reflectance data for the deconvolution of lichen and rock mixtures. *Remote Sens. Environ. 95*, pp. 57-66.

[73] Karnieli, A., Kidron, G.J., Glaesser, C., and Ben-Dor, E., 1999: Spectral characteristics of cyanobacteria soil crust in semiarid environments. *Remote Sens. Environ. 69*, pp. 67-75.

[74] Rees, W.G., Tutubalina, O.V., and Golubeva, E.I., 2004: Reflectance spectra of subarctic lichens between 400 and 2400 nm. *Remote Sens. Environ. 90*, pp. 281-292.

[75] Lange, O.L., Green, T.G.A., Heber, U., 2001: Hydration-dependent photosynthetic production of lichens: what do laboratory studies tell us about field performance? *J. Exp. Bot. 52*, pp. 2033-2042.

[76] Jeffries, D.L., Link, S.O., and Klopatek, J.M., 1993a: CO_2 fluxes of cryptogamic crusts. 1. Response to resaturation. *New Phytol. 125*, pp. 163-173.

[77] Jeffries, D.L., Link, S.O., Klopatek, J.M., 1993b: O_2 fluxes of cryptogamic crusts. 2. Response to dehydration. *New Phytol. 125*, pp. 391-396.

[78] Lange, O.L., Belnap, J., Reichenberger, H., 1998: Photosynthesis of the Cyanobacterial soil-crust lichen Collema tenax from arid lands in southern Utah, USA: role of water content on light and temperature responses of CO2 exchange. *Funct. Ecol. 12*, pp. 195-202.

[79] Karnieli, A., and Tsoar, H., 1995: Spectral reflectance of biogenic crust eeveloped on desert dune sand along the Israel-Egypt border. *Int. J. Remote Sens. 16*, pp. 1741-1741.

[80] Karnieli, A., and Sarafis, V., 1996: Reflectance spectrophotometry of cyanobacteria within soil crusts - A diagnostic tool. *Int. J. Remote Sens. 17*, pp. 1609-1614.

[81] Karnieli, A, Shachak M, Tsoar H, Zaady E, Kaufman Y, Danin A, and Porter W., 1996: The effect of microphytes on the spectral reflectance of vegetation in semiarid regions. *Remote Sens. Environ., 57(2)*, pp. 88-96.

[82] Karnieli, A., 1997: Development and implementation of spectral crust index over dune sands. *Int. J. Remote Sens. 18*, pp. 1207-1220.

[83] Hill, J., Hostert, P., Tsiourlis, G., Kasapidis, P., Udelhoven, T., and Diemer, C., 1998: Monitoring 20 years of increased grazing impact on the Greek island of Crete with earth observation satellites. *J. Arid Environ. 39*, pp. 165-178.

[84] McIntyre, D.S. 1958: Permeability measurement of soil crust formed by raindrop impact. *Soil Sci. 85*, pp. 158-189.

[85] Goldshleger, N., Ben-Dor, E., Benyamini, Y., Blumberg D., and Agassi, M., 2002: Spectral properties and hydraulic conductance of soil crusts formed by raindrop impact. *Int. J. Remote Sens.23*, pp. 3909–3920.

[86] de Jong, S.M., 1992: The analysis of spectroscopical data to map soil types and soil crusts of mediterranean eroded soils. *Soil Technol. 5*, pp. 199-211.

[87] Goldshleger, N., Ben-Dor, E., Benyamini, Y., Agassi, M., and Blumberg ,D.G., 2001: Characterization of soil's structural crust by spectral reflectance in the SWIR region (1.2±2.5 µm). *Terra Nova*, 13, pp. 12-17.

[88] Eshel, G., Levy, G.J., and Singer, M.J., 2004: Spectral reflectance properties of crusted soils under solar illumination. *Soil Sci. Soc. Am. J.68*, pp. 1982-1991.

[89] Courault, D., P. Bertuzzi, P., and M. C. Girard , M.C., 1993:. Monitoring surface changes of bare soils due to slaking using spectral measurements. *Soil Sci. Soc. Am. J.*, 57:1595-1601.

[90] Ben-Dor, E., Goldlshleger, N., Benyamini, Y., Agassi, M., and Blumberg, D.G., 2003: The spectral reflectance properties of soil structural crusts in the 1.2- to 2.5-mu m spectral region. *Soil Sci. Soc. Am. J. 67,* pp. 289-299.

[91] Godschleger, N., Ben-Dor, E., Benyamini, Y., Agassi, M., 2004: Soil reflectance as a tool for assessing physical crust arrangement of four typical soils in Israel. *Soil Sci. 169*, pp. 677-687.

[92] Cooke, R.U., and Warren, A., 1973: Geomorphology in deserts. London: B.T. Batsford Ltd., p. 120.

[93] Dorn, R.I., and Oberlander, T.M., 1981: Microbial origin of desert varnish. *Science 213,* pp. 1245-1247.

[94] Potter, R.M., and Rossman, G.R., 1979: Mineralogy of manganese dendrites and coatings. *Am. Mineral. 64,* pp. 1219-1226.

[95] Dorn, R.I., and Oberlander, T.M., 1982: Rock Varnish. *Progress in Phys. Geograph. 6*, pp. 317-367.

[96] Richardson, A.J. and C.L. Wiegand, 1977: Distinguishing Vegetation from Soil Background Information. *Photogram. Eng and Remote Sens.43*, pp. 1541-1552.

[97] Elvidge, C. D. and Z. K. Chen, 1995: Comparison of Broad-Band and Narrow-Band Red and Near-Infrared Vegetation Indices. *Remote Sens. Environ. 54,* pp.38-48.

[98] Baret, F., Jacquemoud, S., and Hanocq, J. F., 1993: The soil line concept in remote sensing. *Remote Sens. Rev. 7*, pp.65-82.

[99] Fox, G. A., Sabbagh, G.J., Searcy, S.W., and Yang, C., 2004. An Automated Soil Line Identification Routine for Remotely Sensed Images. *Soil Sci. Soc. Am. J. 68,* pp. 1326-1331.

[100] Kokaly, R.F., and Clark, R.N., 1999: Spectroscopic determination of leaf biochemistry using band-depth analysis of absorption features and stepwise multiple linear regression. *Remote Sens. Environ. 67*, pp. 267-287.

[101] Van der Meer, F., 2004: Analysis of spectral absorption features in hyperspectral imagery. *Int. J. Appl. Earth Observ. Geoinform. 5,* pp. 55-68.

[102] Palacios-Orueta, A. and Ustin, S.L., 1998: Remote sensing of soil properties in the Santa Monica mountains: I. Spectral analysis. *Remote Sens. Environ. 65,* pp.170-183.

[103] Whiting, M.L., Palacios-Orueta, A., Li, L., and Ustin, S.L., 2005b: Soil moisture and stratified landscape parameters improve soil mineral mapping with hyperspectral imagery. *Remote Sens. Environ*. (in preperation)

[104] Whiting, M.L., Li, L., and Ustin, S.L., 2004: Predicting Water Content Using Gaussian Model on Soil Spectra. *Remote Sens. Environ., 89*, pp. 535-552.

[105] Clark, R.N., 1999: Spectroscopy of rocks and minerals, and principles of spectrocopy. In: Rencz, A.N. (ed.), Remote Sensing for the Earth Sciences: Manual of Remote Sensing. pp. 3-58. New York: John Wiley & Sons, Inc.

[106] Bowers, S.A., and Hanks, R.J., 1965: Reflection of radiant energy from soils. *Soil Sci. 100*, pp. 130-138.

[107] Lobell, D.B., and Asner, G.P., 2002: Moisture effects on soil reflectance. *Soil Sci. Soc. Am. J. 66*, pp. 722-727.

[108] Liu, W., Baret, F., Gu, X., Tong, Q., Zheng, L., and Zhang, B., 2002: Relating soil surface moisture to reflectance. *Remote Sens. Environ. 81*, pp. 238-246.

[109] Dalal, R. C. and Henry, R.J., 1986: Simultaneous determination of moisture, organic carbon and total nitrogen by near infrared reflectance spectroscopy. *Soil Sci. Soc. Am. J.50*, pp. 120-123.

[110] Aranda, V., and Oyonarte, C., 2005: Effect of vegetation with different evolution degree on soil organic matter in a semi-arid environment (Cabo de Gata-Nijar Natural Park, SE Spain). *J. Arid Environ. 62*, pp. 631-647.

[111] Henderson, T.L., Baumgardner, M.F., Franzmeier, D.P., Stott, D.E., and Coster, D.C., 1992: High dimensional reflectance analysis of soil organic matter. *Soil Sci. Soc. Am. J. 56,* pp. 865-872.

[112] Coleman, T. L. and Montgomery,O.L., 1987: Soil moisture, organic matter, and iron content effect on the spectral characteristics of selected vertisols and alfisols in Alabama. *Photogram. Eng. and Remote Sens. 53,* pp. 1659-1663.

[113] Palacios-Orueta, A. and Ustin, S.L., 1996: Multivariate classification of soil spectra. *Remote Sens. Environ. 57,* pp. 08-118.

[114] Demattê, J.A.M., Pereira, H.S., Nanni, M.R., Cooper, M., and Fiorio, P.R., 2003: Soil chemical alterations promoted by fertilizer application assessed by spectral reflectance. *Soil Sci. 168*, pp.730-747.

[115] Chen, F., Kissel, D.E., West, L.T., and Adkins, W., 2000: Field-scale mapping of surface soil organic carbon using remotely sensed imagery. *Soil Sci. Soc. Am. J. 64*, pp. 746-753.

[116] Metternicht, G.I. and Zinck, J.A., 2003: Remote sensing of soil salinity: potentials and constraints. *Remote Sens. Environ. 85*, pp. 1-20.

[117] Matthias, A.D, Fimbres, A., Sano, E.E., Post, D.F., Accioly, L., Batchily, A.K., and Ferreira, L.G. 2000: Surface Roughness Effects on Soil Albedo. *Soil Sci. Soc. Am. J. 64*, pp. 1035-1041.

[118] Deering, D.W., Eck, T.F., and Otterman, J., 1990. Bidirectional reflectances of selected desert surfaces and their three-parameter soil characterization. *Agr. Forest Meteorol. 52*, pp. 71-93.

[119] Shoshany, M., 1993: Roughness-reflectance relationship of bare desert terrain, an empirical study. *Remote Sens. Environ. 45*, pp. 15-27.

[120] Cierniewski, J. and Karnielli, A., 2002: Virtual surfaces simulating the bi-directional reflectance of semi-arid soils. *Int. J. Remote Sensing 23*, pp. 4019-4037.

[121] Palacios-Orueta, A., Pinzon, J.E., Ustin, S.L., and Roberts, D.A., 1999: Remote sensing of soil properties in the Santa Monica Mountains. II. Hierarchical foreground and background analysis. *Remote Sens. Environ. 68*, pp. 138-151.

[122] Melamed, M.T., 1963: Optical properties of powders. Part I. Optical absorption coefficients and the absolute value of the diffuse reflectance. *J. Appl. Phys.* 34: pp. 560–570.

[123] Mustard, J.F., 1992: Chemical analysis of actinolite from reflectance spectra. *Am. Mineral. 77*, 345-358.

[124] Whiting, M. L., Li, L., and Ustin, S.L., 2005a: Effects of overlapping absorptions on soil mineral content estimates. *Remote Sens. Environ.* (in review).

[125] Clark, R.N., and Roush, T.L., 1984: Reflectance spectroscopy: Quantitative analysis techniques for remote sensing applications. *J. Geophysl Res. 89*, pp. 6329-6340.

[126] Sunshine, J.M., Pieters, C.M., and Pratt, S.F., 1990: Deconvolution of mineral absorption bands - an improved approach. *J. Geophysl Res.-Solid Earth and Planets 95*, pp. 6955-6966.

[127] Huete, A.R., Liu, H.Q., Batchily, K., and van Leeuwen, W., 1997: A comparison of vegetation indices global set of TM images for EOS-MODIS. *Remote Sens. Environ. 59*, pp. 440-451.

[128] Serrano, L., Penuelas, J., and Ustin, S.L., 2002: Remote sensing of nitrogen and lignin in Mediterranean vegetation from AVIRIS data: decomposing biochemical from structural signals. *Remote Sens. Environ. 81*, pp. 355-364.

[129] Pinzóon, J.E., Ustin, S.L., Castañneda, C.M., and Smith, M.O.. 1998: Investigation of leaf biochemistry by hierarchical foreground/background analysis. *IEEE Trans. Geosci. and Remote Sens. 36*, pp. 1-15.

[130] Smith, M-L., Ollinger, S.V., Martin, M.E., Aber, J.D., Halett, R.A., and Goodale, C.L., 2002: Direct estimation of aboveground forest productivity through hyperspectral remote sensing of canopy nitrogen. *Ecol. Appl. 12*, pp. 1286-1302.

[131] Madeira, J., Bedidi, A., Cervelle, B., Pouget, M. and Flay, N. 1997: Visible spectrometric indices of hematite (Hm) and goethite (Gt) content in lateritic soils: the application of a Thematic Mapper (TM) image for soil-mapping in Brasilia, Brazil. *Int. J. Remote Sens. 18*, pp. 13,2835-2852.

[132] Mathieu, R., Pouget, M., Cervelle, B., Escadafal, R., 1998: Relationships between satellite-based radiometric indices simulated using laboratory reflectance data and typic soil color of an arid environment. *Remote Sens. Environ. 66* , pp. 17-28

[133] Allen, W.A., Gausman, H.W., Richardson, A.J., and Thomas, J.R., 1969: Interaction of isotropic light with a compact leaf. *J. Opt. Soc. Am. 59*, pp. 1376-1379.

[134] Allen, W.A., Gausman, H.W., and Richardson, A.J., 1970: Mean effective constants of cotton leaves. *J. Opt. Soc. Am. 60*, pp. 542-547.

[135] Fourty T.H., Baret F., Jacquemoud S., Schmuck G., and Verdebout J., 1996: Optical properties of dry plant leaves with explicite description of their biochemical composition: direct and inverse problems. *Remote Sens. Environ. 56*, pp. 104-117.

[136] Baret, F., and Fourty, T.H., 1997: Estimation of leaf water content and specific leaf weight from reflectance and transmittance measurements. *Agronomie 17*, pp. 455-464.

[137] Fourty, TH., and Baret, F., 1998: On spectral estimates of fresh leaf biochemistry. *Int. J. Remote Sens.19*, pp. 1283-1297.

[138] Ceccato, P., Flasse, S., Tarantola, S., Jacquemoud, S., and Grégoire, J.M., 2001: Detecting vegetation water content using reflectance in the optical domain. *Remote Sens. Environ.* 77, pp. 22-33.

[139] Bacour, C., Jacquemoud, S., Tourbier, Y., Dechambre, M., and Frangi, J.P., 2002: Design and analysis of numerical experiments to compare four canopy reflectance models. *Remote Sens. Environ. 79*, pp. 72-83.

[140] Tucker, C.J., 1979: Red and photographic infrared linear combinations for monitoring vegetation. *Remote Sens. Environ. 8*, pp. 127-150.

[141] FUENTES, D. A., J. A. GAMON, J.A , QIU, H.L., SIMS, D.A., AND ROBERTS, D.A., 2001: Mapping Canadian boreal forest vegetation using pigment and water absorption features derived from the AVIRIS sensor. *J. Geophys. Res. 106*, pp. 33565-33577.

[142] ZARCO-TEJADA, P. J., 1998: Optical indexes as bioindicators of forest sustainability. Graduate Programme in Earth and Space Science. Toronto, York University.

[143] LICHTENTHALER, H.K., LANG, M., SOWINSKA, M., HEISEL, F., AND MIEHE, J.A., 1996: Detection of vegetation stress via a new high resolution fluorescence imaging system. *J. Plant Physiol. 148*, pp. 599-612.

[144] GAO, B.-C., 1996: NDWI - A normalized difference water index for remote sensing of vegetation liquid water from space. *Remote Sens. Environ. 58,* pp. 257-266.

[145] CHUVIECO, E., VENTURA, G., MARTIN, M.P., AND GOMEZ, I., 2005: Assessment of multitemporal compositing techniques of MODIS and AVHRR images for burned land mapping. *Remote Sens. Environ. 94*, pp. 450-462.

[146] CONEL, J.E., AND VAN DEN BOSCH, J., GROVE, C.I., 1993: Application of a two-stream radiative transfer model for leaf lignin and cellulose concentrations from spectral reflectance measurements. Parts 1 & 2. In: R.O. Green (ed): Proc. 4th Annual JPL Airborne Geoscience Workshop. Vol. 1. AVIRIS Workshop 25-29 October 1993, Washington (DC), NASA-JPL Publication 93-26, pp. 39-51.

[147] DAWSON T.P., CURRAN P.J., AND PLUMMER S.E., 1998: LIBERTY - Modelling the effects of leaf biochemical concentration on reflectance spectra. *Remote Sens. Environ. 65*, pp. 50-60.

[148] MA, Q., ISHIMARU, A., PHU, P., AND KUGA, Y., 1990: Transmission, reflection, and depolarization of an optical wave for a single leaf. *IEEE Trans. Geosci. Remote Sens 28*, pp. 865-872.

[149] GANAPOL, B., JOHNSON, L., HAMMER, P., HLAVKA, C., AND PETERSON, D., 1998: LEAFMOD: a new within-leaf radiative transfer model. *Remote Sens. Environ. 6*, pp. 182-193.

[150] JOHNSON, L.F., 2001: Nitrogen influence on fresh-leaf NIR spectra. *Remote Sens. Environ,* 78: pp. 314-320.

[151] TUCKER, C..J. AND GARRATT, M.W., 1977: Leaf optical properties as a stochastic process. *Appl. Opt.16*, pp. 635-642.

[152] MAIER, S.W., LÜDEKER, W., AND GÜNTHER, K.P., 1999: SLOP: A revised version of the stochastic model for leaf optical properties. *Remote Sens. Environ. 68,* pp. 273-280.

[153] HOSGOOD, B., JACQUEMOUD, S., ANDREOLI, G., VERDEBOUT, J., PEDRINI, A., AND SCHMUCK, G., 1994: The JRC Leaf Optical Properties Experiment (LOPEX'93), European Commission, Directorate-General XIII, Telecommunications, Information Market and Exploitation of Research, L-2920, Luxembourg. CL-NA-16095-EN-C.

[154] GOVAERTS, Y.M., JACQUEMOUD, S., VERSTRAETE, M.M., AND USTIN, S.L., 1996: Three-dimensional radiation transfer modeling in a dicotyledon leaf. *Appl. Opt. 35,* pp. 6585-6598.

[155] GOVAERTS, Y.M., AND VERSTRAETE, M.M., 1998: Raytran: A Monte Carlo ray-tracing model to compute light scattering in three-dimensional heterogeneous media. *IEEE Trans. Geosci. Remote Sens. 36*, pp. 493-505.

[156] USTIN S.L., JACQUEMOUD, S., AND GOVAERTS, Y.M., 2001. Simulation of photon transport in a three-dimensional leaf: Implication for photosynthesis. *Plant Cell Environ. 24*, pp. 1095-1103.

[157] BARANOSKI, G.V.G, AND ROKNE, J.G., 2004: Light interaction with plants. A Computer Graphics Perspective, Horwood Publishing.

[158] ZARCO-TEJADA P.J., PUSHNIK J.C., DOBROWSKI S., AND USTIN S.L., 2003a: Steady-state Chlorophyll a fluorescence detection from canopy derivative reflectance and double-peak effects. *Remote Sens. Environ. 84,* pp. 283-294.

[159] DOBROWSKI, S.Z., PUSHNIK, J.C., ZARCO-TEJEDA, P.J., AND USTIN, S.L., 2005: Simple reflectance indicesindexes track heat and water stressed induced changes in steady state chlorophyll fluorescence at the canopy scale. *Remote Sens. Environ. 97,* pp. 403-414.

[160] MILLER, J.R., BERGER M., GOULAS Y., JACQUEMOUD S., LOUIS J., MOISE N., MOHAMMED G., MORENO J., MOYA I., PEDRÓS R., VERHOEF W., AND ZARCO-TEJADA P.J., 2005: Development of a Vegetation Fluorescence Canopy Model, ESTEC Contract No. 16365/02/NL/FF, Final Report, May 2005 (http://www.ias.csic.es/fluormod/)

[161] PEDRÓS R., GOULAS Y., JACQUEMOUD S., LOUIS J., AND MOYA I., 2005: A new leaf fluorescence model. Part 1: Fluorescence excitation & Part 2: Fluorescence emission, *Remote Sens. Environ.*, forthcoming.

[162] GOND, V., FONTES, J., LOUDJANI, J.P., 1997: African biomes dynamic by remote sensing temporal analysis. *Comptes Rendus De L'Academie Des Sciences Serie III-Sciences De La Vie-Life Sciences 320*, 179-188

[163] ALT C., STUTZEL, H., AND KAGE, H., 2000: Optimal nitrogen content and photosynthesis in cauliflower (*Brassica oleracea L. botrytis).* Scaling up from leaf to whole plant. *Ann. Bot.-London 85*, pp. 779-787.

[164] FIELD, C., and MOONEY, H.A., 1986. The photosynthesis-nitrogen relationship in wild plants. In: Givinsh, T.J. (ed.): On the economy of form and function, pp. 25–55. Cambridge University Press, Cambridge,

[165] GARNIER, E., SALAGER, J.L., LAURENT, G., SONIE, L., 1999: Relationships between photosynthesis, nitrogen and leaf structure in 14 grass species and their dependence on the basis of expression. *New Phytol. 143*, pp. 119-129.

[166] BOUSQUET, L., LACHERADE, S., JACQUEMOUD, S., AND MOYA, I., 2005: Leaf BRDF measurement and model for specular and diffuse component differentiation. *Remote Sens. Environ.* (in press).

[167] LUQUET, D., BEGUE, A., DAUZAT, J., NOUVELLON, Y., REY, H., 1998. Effect of the vegetation clumping on the BRDF of a semi-arid grassland: comparison of the SAIL model and ray tracing method applied to a 3D computerized vegetation canopy, in Proc. Geoscience and Remote Sensing Symposium (IGARSS '98), 6-10 July 1998, pp. 791-793.

[168] PINTY, B., VERSTRAETE, M.M., IAQUINTA, J. AND GOBRON, N., 1996: Advanced modelling and inversion techniques for the quantitative characterization of desertification. In: Proc. The use of remote sensing for land degradation and desertification monitoring in the Mediterranean bassin, EN, Valencia (Spain), 13-15 June 1994, European Commission, Vol. EUR 16732, pp. 79-93.

[169] ESTEVE, P., FONTES, J., GASTELLU-ETCHEGORRY, J.P., 1998: Tropical dry ecosystems modelling and monitoring from space. *Ecol. Model. 108*, pp. 175-188.

[170] GASTELLU-ETCHEGORRY, J.-P., DEMAREZ, V., PINEL, V., AND ZAGOLSKI, F., 1996: Modeling radiative transfer in heterogeneous 3-D vegetation canopies. *Remote Sens. Environ. 58*, pp. 131-156.

[171] ZARCO-TEJADA, P.J., RUEDA, C.A., AND USTIN, S.L., 2003: Water content estimation in vegetation with MODIS reflectance data and model inversion methods. *Remote Sens. Environ. 85*: pp. 109-124.

[172] WIDLOWSKI, J.L., PINTY, B., GOBRON, N., VERSTRAETE, M.M., AND DAVIS, A.B., 2001: Characterization of surface heterogeneity detected at the MISR/TERRA subpixel scale. *Geophys. Res. Lett. 28*, pp. 4639-4642.

[173] STONER, E.R. AND BAUMGARDNER, M.F., 1981: Characteristic variations in reflectance of surface soils. *Soil Soil Sci. Soc. Am. J. 45*, pp. 1161-1165.

[174] HENDERSON, T.L., SZILAGYI, A., BAUMGARDNER, M.F., CHEN, C-C.T., AND LANDGREBE, D.A., 1989: Spectral band selection for classification of soil organic matter content. *Soil Sci. Soc. Am. J. 53*, pp. 1778-1784.

[175] ESCADAFAL, R., BELGHITH, A., AND BEN MOUSSA, H. 1994: Indices spectraux pour la degradation des milieux naturels en Tunisie aride. 6éme Symp. Int. Mesures Physiques et Signatures en Télédétection., Val d'lsère, France, ISPRS-CNES.

[176] ESCADAFAL, R. AND A. HUETE, 1991: Etude des propriétés spectrales des sols arides appliquée à l'amélioration des indices de végétation obtenus par télédétection. *C. R. Acad. Sci. Paris 312*, pp. 1385-1391.